Impact of mid-to-late Holocene precipitation changes on vegetation across lowland tropical South America: a palaeo-data synthesis

Impact of mid-to-late Holocene precipitation changes on vegetation across lowland tropical South America: a paleo-data synthesis

Authors: Richard J. Smith[a1] and Francis E. Mayle[a]

Affiliations:

[a] University of Reading, Centre for Past Climate Change and Department of Geography & Environmental Science, School of Archaeology, Geography and Environmental Science (SAGES), Whiteknights, PO Box 227, Reading RG6 6AB, UK

[1]Correspondence to: r.smith3@pgr.reading.ac.uk

ABSTRACT

A multi-proxy paleo-data synthesis of 110 sites is presented, exploring the impact of mid-to-late Holocene precipitation changes upon vegetation across Southern Hemisphere tropical South America. We show that the most significant vegetation changes occurred in south-west Amazonia and south-east Brazil, regions reliant on precipitation derived from the South American summer monsoon (SASM). A drier mid Holocene in these regions, linked to a weaker SASM, favoured more open vegetation (savannah/grasslands) than present, while increased late-Holocene precipitation drove expansion of humid forests (e.g. evergreen tropical forest in south-west Amazonia, *Araucaria* forests in south-east Brazil). The tropical forests of central, western and eastern Amazonia remained largely intact throughout this 6000-year period. North-eastern Brazil's climate is 'antiphased' with the rest of tropical South America, but a lack of paleo data limits our understanding of how vegetation responded to a wetter(drier) mid(late) Holocene. From this paleo-data perspective, we conclude that ecotonal forests already close to their climatic thresholds are most vulnerable to predicted future drought, but the forest biome in the core of Amazonia is likely to be more resilient. Of greater concern is widespread deforestation and uncontrolled anthropogenic burning, which will decrease ecosystem resilience, making them more vulnerable than they might be without current anthropogenic pressures.

KEYWORDS

Amazonia; tropical South America; Holocene; climate change; paleoecology; data synthesis

INTRODUCTION

The response of the vegetation across tropical South America to long-term climate change is of great concern, given the importance of the ecosystem services this region provides. Of particular concern is how vegetation will respond to a drier climate, given the future projections of more intense dry seasons and increased frequency of severe drought events (Joetzjer et al., 2013; Boisier et al., 2015; Duffy et al., 2015). The extensive work carried out by the RAINFOR ecological monitoring project (Malhi et al., 2002) has demonstrated the short-term vulnerability of Amazonian forests to severe drought events (Phillips et al., 2009; Doughty et al., 2015; Feldpausch et al., 2016). However, whilst the effects of these short-term severe drought events are relatively well understood (e.g. Rowland et al., 2015), considerable uncertainty exists as to how long-term climate change will affect the vegetation of tropical South America. Results of future model simulations using process-based dynamic global vegetation models (DGVMs) range from catastrophic large-scale Amazonian forest die-back as a result of positive feedbacks between the biosphere and atmosphere (Cox et al., 2000; 2004), to other studies suggesting that the forests will be resilient to climate change (Cowling and Shin, 2006; Huntingford et al., 2013). One problem in predicting future vegetation dynamics is the lack of direct long-term observational data of vegetation responses to long-term climate change in the past. However, the use of proxy-based vegetation reconstructions allows us to extend our observational period back millennia through times of significant, long-term climate change. The role of paleoecology in increasing our understanding of long-term vegetation dynamics is well established within the paleo-data community, and is playing an increasingly important role in helping to understand mechanisms and uncertainties within model simulations through initiatives such as PMIP (Paleoclimate Modelling Intercomparison Project) (Joussaume and Taylor, 1995; Braconnot et al., 2011).

Several mid-late Holocene paleoecological syntheses have been undertaken in the past, but these are now relatively outdated (e.g. Mayle and Power, 2008; Marchant et al., 2009) due

to the publication of both new paleoecological and paleoclimate records over the past decade. Furthermore, more recent syntheses (e.g. Prado et al., 2013b; Flantua et al., 2016) have used paleoecological data (predominantly pollen) to reconstruct past climate, which precludes examination of vegetation-climate relationships. We therefore present an updated multi-proxy synthesis of published paleoecological records from across lowland tropical South America from the mid Holocene (ca. 6000 years ago, 6 ka) to the present. This time period is important both paleoecologically and paleoclimatologically, as there is widespread evidence that millennial-scale changes in insolation (driven by the precessional cycle of Earth's orbit) caused long-term precipitation changes, and associated vegetation changes, across the region (Mayle and Power, 2008; Prado et al., 2013a; Baker and Fritz, 2015). Therefore, we will consider the paleoecological records alongside key paleoclimate records from across the study region in order to assess any vegetation changes in the context of long-term climate change.

This synthesis will provide new insights into the spatio-temporal dynamics of biome-scale vegetation changes on a sub-continental scale over the past 6000 years, in the context of climate change inferred from independent paleoclimate data. Although there is increasing evidence that pre-Columbian (pre-AD1492) peoples managed the floristic composition of their forest resources (especially by promoting palms, e.g. Watling et al., 2017), there is little evidence, to date, that they practiced large-scale deforestation. We therefore expect natural drivers (i.e. climate change) to be the most likely explanation for any biome-scale vegetation shifts over the broad, regional scales that we consider in this synthesis – an assumption borne out by a recent study of local-scale human land use nested within regional-scale, climate-driven, forest-savannah biome turnover (Carson et al., 2014). However, if the vegetation history of a given site(s) is inconsistent with independent paleoclimate data from the area, we will consider whether human land use can reconcile this apparent vegetation-climate mismatch.

Modern environmental setting

Modern climatic setting

Figure 1 shows long-term mean precipitation over South America for austral winter (June, July, August, Fig. 1a) and austral summer (December, January, February, Fig. 1b), along with mean wind speed and direction at 850 mb. The relatively narrow, longitudinally orientated belt of precipitation over the tropical oceans marks the location of the Intertropical Convergence Zone (ITCZ). The ITCZ refers to a band of low pressure and convergence of the moist trade winds over the equatorial oceans and is associated with rising air and intense convective precipitation. The rising air at the ITCZ diverges polewards when it nears the tropopause, and descends when over the subtropics, causing semi-permanent high pressure cells over the subtropical oceans such as the South Atlantic subtropical high (SASH – Fig. 1); this loop of air movement is known as the Hadley cell circulation (Garreaud et al., 2009). The different thermal properties of the continental land mass of South America and the surrounding oceans gives rise to a distinct seasonal cycle of precipitation over most of the tropical South American continent. During austral winter, when the thermal equator and ITCZ are located further north, maximum precipitation over the continent is located in northern South America, whereas central South America experiences it's dry season (Fig. 1a). Southern Brazil maintains an important source of moisture from both moist winds fed into the region by the circulation of the SASH and extra-tropical frontal systems (Cruz et al., 2006; Garreaud et al., 2009). During austral spring/summer the thermal equator moves south and heats the central South American land mass up relative to the surrounding oceans. This continental heating causes areas of intense convection to form over central Brazil and southern Amazonia, which are fed with moist easterly trade winds blowing in from the Atlantic Ocean, helped by an intensified SASH. This marks the onset of a system commonly referred to as the South American Summer Monsoon (SASM) (Fig. 1b - Zhou and Lau, 1998; Raia and Cavalcanti, 2008; Silva and Kousky, 2012). As the moist easterly trade winds reach the Andean mountain range, they are diverted southward and are intensified by an area of deep low pressure that forms over the Gran Chaco region (the 'Chaco Low'). This

flow creates a feature known as the South American Low Level Jet (SALLJ), associated with very strong low-level winds that are channelled southwards by the eastern Andes and the Brazilian planalto highlands (Marengo et al., 2002). The SALLJ helps to transport moisture from Amazonia into subtropical south-east Brazil where the South Atlantic Convergence Zone (SACZ) is intensified (Carvalho et al., 2004).

In contrast to the central and southern areas of tropical South America, the north-east of Brazil is conspicuously dry throughout most of the year (Garreaud et al., 2009). The intense updrafts in the central part of the continent (in particular the Chaco Low) during the mature phase of the SASM requires compensating subsidence in surrounding regions. This subsidence manifests as an upper tropospheric low pressure feature called the 'Nordeste Low', which suppresses rainfall over the region of north-east Brazil (Chen et al., 1999; Cruz et al., 2009). This east-west difference in precipitation caused by zonal overturning circulations has been referred to as the east-west South American precipitation dipole (Cheng et al., 2013). Interannual variability in precipitation over tropical South America is linked to the El Niño Southern Oscillation (ENSO); during El Niño episodes, precipitation rates are below average across eastern Amazonia and north-eastern Brazil (Garreaud et al., 2009).

Modern vegetation setting

The lowlands of tropical South America support a wide variety of ecoregions, ranging from humid rainforests to xeric scrublands (Fig. 2a). The ecoregions described here refer to the *potential* ecoregions, as the *actual* vegetation cover has been highly affected by modern deforestation, agriculture and industrialisation. The Amazon humid evergreen tropical forest (HETF) is the largest biome of tropical South America, covering most of northern and western Brazil and extending into neighbouring countries to the west and north where annual precipitation is high (>1600 mm). The southern and eastern ecotonal margins of the Amazon HETF exist in a much more seasonal climate with longer dry seasons. Small

patches of savannah can occur within the Amazon HETF where edaphic conditions are favourable (Adeney et al., 2016). Along the foothills of the Andes lies a band of Yungas forest, a transitional area ranging from moist evergreen lowland forest to montane forests. The Atlantic forest biome, supporting a mix of lowland and montane evergreen forests, exists on the east coast of Brazil where coastal and orographic rainfall maintain a moist climate (Fig. 2c). The *Araucaria* moist forest biome (characterised by the high abundance of the evergreen tree *Araucaria angustifolia*) exists on the highlands of southern Brazil where annual precipitation is high (~2000 mm) and there is a short dry season (< 2 months) (Hueck, 1953; Behling and Pillar, 2007).

In between the Amazon and Atlantic rainforests exists the 'dry diagonal' (Prado and Gibbs, 1993). This is a large area, characterised by highly seasonal rainfall, that contains a mixture of deciduous and semi-deciduous trees, shrubland and savannah. Most of this area is covered by the Cerrado savannah biome. Due to the variety of climatic, edaphic and topographic features in the region, the savannah types range from open grassland to more dense shrub and savannah tree cover (Silva and Bates, 2002). Gallery forests can occur along the streams that flow through the Cerrado, as well as small patches of closed canopy deciduous and semi-deciduous trees where edaphic conditions are favourable (Silva and Bates, 2002; Werneck, 2011). Larger areas of semi-deciduous tropical dry forests (SDF) exhibit a fragmentary distribution. 'Nuclei' of SDF exist across: the Chiquitano region of eastern lowland Bolivia; across southern Brazil along the Paraná and Paraguay rivers and into the Misiones province of northern Argentina; and inland areas of the Atlantic forest biome. SDF exist in highly seasonal climates, with annual precipitation <1600 mm and a dry season length of ~5 – 6 months (Gentry, 1995; Werneck, 2011). These SDF areas exist under similar climatic conditions to the Cerrado savannah, but are restricted to soils with higher nutrient content and high pH (Pennington et al., 2000; Werneck, 2011). The Caatinga region of north-eastern Brazil supports a complex mosaic of xerophytic vegetation types that range from dense SDF cover, more open tree cover with a shrubby sub-canopy, to open

thorn scrubland and savannah. The semi-arid climate is the main control upon this Caatinga vegetation; precipitation rates are low and erratic meaning that long periods of drought are common (Sampaio, 1995). However, small ‘islands’ of humid evergreen rainforest and semi-deciduous tropical dry forests do exist on isolated plateaus inland and near the coast where orographic and coastal rainfall can maintain a humid microclimate (Sampaio, 1995; Montade et al., 2014).

METHODS

A database of 110 paleoecological sites from 87 previously published papers was created through literature searches and interrogation of repositories such as the Latin American Pollen Database (LAPD - Flantua et al., 2015) and Neotoma (http://www.neotomadb.org) (Table 1). This synthesis considers sites from the Southern Hemisphere tropical lowlands, extending into the subtropics of south-east Brazil (a latitudinal range extending from the equator to 30°S)(Fig. 2). We do not include coastal mangrove sites, as vegetation changes at these sites are predominantly driven by sea level change (e.g. Behling et al., 2001b; Guimarães et al., 2012; 2013b; Lorente et al., 2014). For each paleoecological site, we assign a vegetation classification at 500-year time slices from the mid Holocene (6 ka) to the present, based on a critical evaluation of the authors' interpretations of the proxy data. The broad scale vegetation classifications we use are outlined in Table 2. A 'mosaic' classification (a combination of any two vegetation types) was used when interpretation suggests that the vegetation cover at a site was most likely a mixture of vegetation types. Ideally, a site will cover the whole period from 6 ka to the present, although there are a number of sites that cover a shorter period. It does not seem appropriate to ignore sites that do not quite cover the whole period as they may still provide valuable information about vegetation trends in a particular area. Therefore, the sites included in our synthesis must have a vegetation reconstruction spanning from earlier than 4 ka, up to at least 2 ka; this ensures that the sites cover a period where there is strong evidence that the region underwent long-term climate change.

Imposing strict criteria on the chronological quality of each site is problematic in this research area. Sedimentation rates are highly variable between samples; sites with low sedimentation rates are particularly problematic as a relatively short core could encompass many millennia. Sub-sampling resolution also varies between sites depending on the length of the record and the specific research questions of the authors. The paucity of sites across tropical South America means that rejecting sites based on low chronological resolution

would result in only a handful of sites being considered. Therefore, we have been relatively flexible in our consideration of sites with lower chronological resolution; this means that this synthesis can only provide an overview of the broad scale vegetation trends in the region over the last 6000 years, rather than exact timings of any changes. Where possible, calibrated radiocarbon dates and age-depth models that are presented in the original paper(s) of each site are used to inform the timings of any changes at that site. If a site records key vegetation changes through its record but does not present calibrated dates or an age-depth model, we use the Bacon age-depth model v2.2 in R (Blaauw and Christen, 2011) to produce an independent age-depth model for that site using the raw chronological data from the paper. This is the case with 26 of the sites, indicated in Table 1. The IntCal13 calibration curve (Reimer et al., 2013) was chosen over SHCal13 (Hogg et al., 2013), given the hydrological links of the study area with the northern hemisphere (through the SASM and ITCZ).

We acknowledge that other more quantitative methods of classifying vegetation from paleoecological data are available, such as Biomisation (Prentice et al., 1996; Prentice and Webb, 1998) and the REVEALS/LOVE Landscape Reconstruction Algorithm (Sugita, 2007a; 2007b). However, these methods are based predominantly on pollen data from lakes, require access to the raw data of each site, and, in the case of REVEALS, require a high density of sites of multiple sizes in a given area. Furthermore, the REVEALS model has yet to be proven in a Neotropical setting where important assumptions about anemophily are violated by most taxa. The paucity of pollen sites that extend back to the mid-Holocene in our research area limits the usefulness of these quantitative methods (which focus solely on pollen data) in producing a thorough synthesis. For example, in the most recent application of the Biomisation method across Latin America (Marchant et al., 2009), there are only around 24 pollen records in our research area that date back to the mid Holocene. Our method allows us to consider other vegetation proxies in addition to pollen (e.g. phytoliths, stable carbon isotopes) and other paleoecological archives in addition to lakes (e.g. soil

pits), thus increasing the number of sites we can include in our synthesis by utilising the full suite of paleovegetation data available. In addition, our method allows us to take advantage of the in-depth knowledge that the author(s) will have about their site (e.g. pollen taphonomy, catchment), which is lost when using a standardised objective method.

Proxy types

This synthesis includes a variety of paleoecological proxy types, all of which have strengths and limitations that must be considered. The two most common proxy types in this synthesis are fossil pollen and stable carbon isotopes ($\delta^{13}C$). Fossil pollen analysis is the most widely used paleovegetation proxy as it gives a direct indication of what vegetation was growing in an area at a given time. However, care must be taken in interpreting a fossil pollen record as pollen loading into a basin does not necessarily reflect the true vegetation assemblage in the catchment area due to previously mentioned taxonomic-differences in pollen productivities and dispersal characteristics. Additionally, the taxonomic resolution of pollen is highly variable; very few are identifiable to species level, some are identifiable to genus level, and many are only identifiable to family level. These issues mean that reliable interpretation of fossil pollen records is dependent upon modern 'pollen rain' studies whereby pollen traps are left in an area for a set time, after which the pollen assemblages are compared with floristic inventories to determine pollen-vegetation relationships (e.g. Behling et al., 1997; Bush and Rivera, 2001; Gosling et al., 2005; 2009; Jeske-Pieruschka et al., 2010; Guimarães et al., 2014). Stable carbon isotope fractionation ($\delta^{13}C$) utilises the fact that C_3 vegetation (woody plants) and C_4 vegetation (savannah grasses and sedges) have distinct $\delta^{13}C$ carbon isotope signatures (Boutton, 1996; Pessenda, 2004). Whilst this differentiation between C_3 and C_4 vegetation is quite broad, it does reveal whether the landscape was closed-canopy forest or open savannah, especially if bolstered by knowledge of the modern isotopic-vegetation relationships in a given area. We also include a small number of sites with phytolith (plant silica bodies)-based vegetation reconstructions (Piperno, 2006). Unlike

pollen, phytoliths preserve well in oxidised environments (e.g. soils) and are particularly useful in increasing the taxonomic resolution of grass. Although few phytolith-based paleoecological studies have yet been undertaken, recent studies have shown the effectiveness of phytoliths in distinguishing between modern tropical ecosystems in the Amazon (Dickau et al., 2013; Watling et al., 2016).

Several other proxies can provide important complementary information for pollen, $\delta^{13}C$, and/or phytolith studies. Charcoal analysis is commonly used to reconstruct past fire activity, which can be an indication of past changes in climate and vegetation characteristics (Power et al., 2008). Isotopic analysis of nitrogen ($\delta^{15}N$) and chemical analyses of carbon/nitrogen (C/N) ratios can indicate whether the organic matter in a sediment record originates from an aquatic source (elevated levels of ^{15}N, low C/N ratios) or a terrestrial source (low levels of ^{15}N, high C/N ratios) (Meyers, 1994; Horák et al., 2011). Measurements of chemical element concentrations, using methods such as X-ray fluorescence (XRF), can reveal catchment erosion which in turn may be linked to local/regional environmental change.

Archive types and spatial scale of reconstructions

When drawing paleoecological inferences from vegetation proxy data, it is important to consider the spatial scale that the latter represents. This spatial scale is influenced by both the type of proxy, as well as the size and type of deposit that the proxy came from. It is widely accepted in the field of palynology that the spatial scale represented by pollen assemblages in lake sediments is related to the size of that lake; small lakes (and bogs) represent local-scale vegetation, whereas large lakes represent regional-scale vegetation (Davis, 2000). This relationship has been shown through practical experiments that correlate pollen signals from lake surface-sediment samples to vegetation inventories at increasing distances from the lake, as well as being formerly quantified in a pollen deposition/dispersal model (Prentice, 1985; Sugita, 1993; 1994). Whilst most of this research has been done for

mid to high latitudes, the pattern is expected to be valid for the tropics. Soil pits are a common archive type that usually use $\delta^{13}C$ isotope as a paleoecological proxy (and in some cases phytoliths). These records essentially represent a 'point' scale (i.e. a record of the vegetation that grew directly in that soil) and as such transects/networks of soil pits are often taken to help represent a larger spatial area. For this synthesis, we categorise each site into one of 4 archive types: lakes, peat bogs, terrestrial (e.g. unspecified sediment hollows or swamps) and soil pits. In an attempt to visually represent the spatial scale that each record represents, we display different sized circles in Figure 4 based on the rules defined in Table 3. In some cases, the display of soil profiles that are very close together have been combined; this has been indicated in Table 1 whenever this is the case.

Paleoclimate records

To assess the relationship between vegetation change and long-term climate change, we have selected 8 key paleoclimate records from across the region (Figs. 2 and 3). Five of these sites (El Condor, Tigre Perdido, Huaguapo, Botuvera Cave and Rio Grande do Norte) have precipitation reconstructions based on speleothem stable oxygen isotope ($\delta^{18}O$) records, while precipitation records of the other sites are based upon lake-level reconstructions (Lake Titicaca and Laguna La Gaiba) or $\delta^{18}O$ analyses of lake calcite deposits (Lake Junin). As with the paleoecological records, we rely upon the authors' expert knowledge of these sites to inform our interpretations. This is particularly important for the speleothem records, as changes in isotopic composition can be influenced by a number of factors, including changes in moisture source, temperature, and/or rainfall amount (Lachniet, 2009).

SYNTHESIS AND DISCUSSION

Figure 4 shows the paleovegetation reconstruction for each site at 500-year time slices from 6 ka to present. Figure S1 in the supplementary information provides a summary of the changes at each site for each area defined in Figure 2. Our discussion of these paleovegetation records is divided into the areas defined in Figure 2, within the context of precipitation changes inferred from key paleoclimate records from across the study area (Figure 3). The main mechanism for these millennial scale precipitation changes has been attributed to changes in austral summer insolation driven by the precessional cycle of Earth's orbit. During the mid Holocene, lower austral summer insolation levels caused a northward shift in the mean position of the ITCZ (Haug et al., 2001) and a decrease in intensity of the SASM (Cruz et al., 2005; Wang et al., 2007; Vuille et al., 2012). In addition, lower austral summer insolation during the mid-Holocene dampened ENSO activity and reduced associated interannual variability of rainfall associated with El Niño/La Niña events (Moy et al., 2002; Koutavas and Joanides, 2012). Individual interpretations of the paleoclimate records will be drawn upon in the sections below.

Central and western lowland Amazonia (CW)

Speleothem records from the western Peruvian Amazon show slightly elevated $\delta^{18}O$ values at the mid-Holocene (Fig. 3 a-b). This finding suggests that convective precipitation may have been slightly reduced at this time, consistent with a weakened SASM linked to lower summer insolation (Haug et al., 2001; van Breukelen et al., 2008). However, an overall reduction in total rainfall amount across western lowland Amazonia was probably relatively small due to mechanisms such as the important source of moisture from transpiration processes across central and eastern Amazonia (Eltahir and Bras, 1994; Spracklen et al., 2012; Cheng et al., 2013). The paleovegetation records support the idea that moisture levels have been relatively stable in this region from 6 ka to present. The sites from across central and western lowland Amazonia show that the HETF biome stayed largely intact in this region throughout the mid-to-late Holocene. Evidence of this biome stability comes from

consistent HETF pollen signals from large lake sites (reflecting regional scale vegetation signals - e.g. Behling et al., 2001c; Horbe et al., 2011) and small sites (reflecting local vegetation signals - e.g. Liu and Colinvaux, 1988; Behling et al., 1999; Bush et al., 2004b). Even if moisture levels were slightly lower during the mid-Holocene, it is clear this was not enough to cause biome turnover. This is currently one of the wettest parts of tropical South America (annual precipitation >3000 mm Fig. 2c) with little or no dry season, therefore precipitation levels would have to reduce drastically to cause widespread forest die-back or biome turnover.

South-Western Amazonia (SW)

The area of south-western Amazonia contains the modern ecotonal boundary between the southern Amazonian HETF, the Chiquitano SDF and the Cerrado savannah (Fig. 2a). Precipitation levels in this region are highly dependent on the strength of the SASM, especially with regards to the development of the Chaco low and the SALLJ that help to divert precipitation from central Amazonia along the Andes and southwards into eastern Bolivia. As a result, this area has a modern precipitation regime that is much more seasonal than that of the central Amazon basin, with longer dry seasons and lower total annual precipitation of ~1500-1600 mm (Fig. 2c). Therefore, the HETF that grows here is much closer to it's climatic limit and is more likely to be sensitive to even small changes in precipitation. During the mid Holocene, paleoclimate records from the high Andes suggest this region was drier than present (Fig. 3 c-e). Although these records come from the high Andes, they can be considered as representative of lowland south-west Amazonia, at least in regards to the direction of precipitation changes, as they too are dependent on the components of the SASM to divert moisture from central Amazonia. Lake levels at Lake Titicaca on the Bolivian altiplano were ~100m lower than modern at 6 ka (Baker et al., 2001), and enriched $\delta^{18}O$ values from the Huaguapo speleothem and Lake Junin suggest reduced convective activity and lower moisture levels (Seltzer et al., 2000; Kanner et al., 2013). These Andean records show that modern levels of precipitation were not reached until ca. 4

– 3 ka. A similar pattern of increasing precipitation through the mid-to-late Holocene is found in the paleoclimate record from the lowland site of Laguna La Gaiba (LLG, Fig. 3f), although this record suggests that modern moisture levels perhaps were not reached here until ca. 2.5 – 2 ka. Overall, the signals from these sites are consistent with the explanation of a gradual increase in SASM strength in response to increased insolation through the mid-to-late Holocene (Burbridge et al., 2004; Kanner et al., 2013; Baker and Fritz, 2015). The time delay between the Andean records and LLG reaching modern levels could suggest a lag between precipitation increasing in the Andean highlands and in the south-west Amazonian lowlands.

Two key lake sites, Laguna Bella Vista (LBV, id = 6) and Laguna Chaplin (LCH, id = 7), provide strong evidence of vegetation shifts through the mid-to-late Holocene in response to the changes in precipitation (Mayle et al., 2000; Burbridge et al., 2004). These are very large lakes (> 3 km diameter) and so their pollen assemblages are assumed to represent regional scale vegetation signals. They currently lie in HETF, 130 km (LBV) and 30 km (LCH) north of the modern HETF/SDF/savannah ecotone. However, during much of the mid-to-late Holocene (ca. 6 ka to 2 ka) a mosaic of SDF/savannah vegetation dominates the catchment of these lakes, providing evidence that the HETF/SDF/savannah ecotone was at least 130 km further north than at present. This SDF/savannah mosaic is persistent in the area until ca. 2 ka, when HETF expanded southward into the catchment of LBV; it is not until ca. 1 ka when HETF reached the catchment of LCH. Another large lake record (Laguna Oricore, id = 5), located 200 km to the west of LBV, shows a consistent pattern of a SDF/SAV dominated landscape changing to HETF at ca. 2 ka (Carson et al., 2014). The two small sites near to Oricore record a later expansion of HETF at ca. 0.5 ka, but this delay has been attributed to pre-Columbian human land management by the authors (Carson et al., 2014; 2016). To the east of these records on the eastern edge of the Chiquitano SDF, the regional pollen record from Laguna La Gaiba (id = 8) suggests that there was no significant contraction of the SDF biome associated with mid-Holocene drought (Whitney et al., 2011). Around 600 km north of

LBV lies a series of natural savannah ‘islands’ located within the dense Amazon rainforest. Evidence that these savannah islands expanded by ~60 km at the expense of HETF during the mid Holocene comes from $\delta^{13}C$ data from a 200 km transect of soil pits between Porto Velho and Humaita (de Freitas et al., 2001; Pessenda et al., 2001), spanning the savannah islands. A contemporaneous drying out of a nearby bog (Cohen et al., 2014), together with the 100 m lowstand in Lake Titicaca in the high Andes (Baker et al., 2001) suggests that a drier climate likely drove these savannah island expansions. The subsequent contraction of these savannah islands began between ca. 2.5 and 2 ka, with modern $\delta^{13}C$ values reached by ca. 1.5 ka, concurrent with the forest expansion seen in north-eastern Bolivia (Mayle et al., 2000).

A weaker SASM in the mid Holocene is likely to have increased the length and severity of the dry season, and decreased annual precipitation below the ~1500 mm climatic threshold between HETF and SDF/SAV, thus driving the northward ecotonal movement. The resilience of the SDF in the eastern Chiquitano region suggests that climate was not sufficiently dry to cause a drastic vegetation shift to dry savannah/scrubland or Caatinga-type vegetation such as that seen in the modern nordeste region of Brazil. Severe drought events were likely more common, which would have favoured the opportunistic expansion of the savannah vegetation into the vulnerable areas of HETF in the savannah island region, perhaps aided by more frequent fire events. The ca. 1000-year time lag between HETF expansion at LCH versus LBV could reflect the latitudinal time-transgressive nature of precipitation increase, and/or a degree of hysteresis in vegetation response (Burbridge et al., 2004). It is important to note that sites from the western Bolivian/south-eastern Peruvian Amazon show stability of HETF through the last 6000 years (Bush et al., 2004b; 2007b; Urrego et al., 2013). This area receives more precipitation than eastern Bolivia, partly due to it’s location on the Andean flank and the associated orographic rainfall (Killeen et al., 2007). Even if moist winds associated with the SASM and SALLJ were reduced in the mid

Holocene, the orographic processes are still likely to have maintained a moist windward Andean flank (Killeen et al., 2007; Urrego et al., 2013).

South-Eastern Brazil (SB)

South-eastern Brazil marks the 'exit region' of the SASM; during the mature phase of the SASM moisture is transported from central Amazonia to this region via the SALLJ – helped by the Chaco Low and the channelling of the Andes and south Brazilian highlands (Fig. 1b). The speleothem records from Botuvera Cave (Wang et al., 2007; Bernal et al., 2016) provide evidence that this region was drier during the mid-Holocene as less moisture was being received from the Amazon Basin (Fig. 3g), consistent with the paleoclimate records from the Andes (Baker et al., 2001) and the interpretation of a weaker SASM in response to lower austral summer insolation. The enhancement of moisture transport from the Amazon Basin into south-east Brazil is recorded from ca. 4 ka, around the same time that precipitation levels are shown to increase in the Andean speleothem records. Modern moisture levels were not reached until ca. 2 to 1.5 ka. Bernal et al. (2016) note that even though the region receives moisture from extratropical sources, the changes in total rainfall for south-eastern Brazil during the mid-to-late Holocene were predominantly driven by insolation changes and associated SASM intensity.

The paleovegetation records from south-eastern Brazil suggest that open vegetation was more widespread at 6 ka, with increases in arboreal vegetation types through to the present. However, given the diverse range of landscapes in this region, it is unsurprising to find that the timing, magnitude and type of forest expansion is highly variable between different areas. The sites located in the SDF region in the SE Brazilian state of Minas Gerais suggest that this area of SDF remained largely intact through the mid-to-late Holocene. This pattern is exemplified by the reconstructions from two large lakes in the core of this area of SDF, Lago Silvana (id = 9, Rodrigues-Filho et al., 2002) and Dom Helvecio (id = 10, Ybert et al., 2000; Turcq et al., 2002), that show consistent SDF pollen signals, depleted $\delta^{13}C$ and low

451 erosional rates throughout the last 6 ka. However, records from smaller sites do reveal more
452 localised vegetation changes from increased SAV in the mid-Holocene (6 ka) to an increase
453 in SDF cover between ca. 5 – 4 ka and again in the last ca. 1 ka. These timings are roughly
454 consistent with the precipitation pattern interpreted from the Botuvera Cave speleothem.
455 Development of dry forest occurred near the borders of the Misiones SDF region from ca. 2
456 – 1 ka (Pessenda, 2004; Zech et al., 2009). This SDF expansion suggests that whilst the
457 mid-Holocene climate was not dry enough to cause biome turnover from SDF to savannah,
458 there was sufficient drying, due to an increase in dry season length, to cause an opening of
459 more marginal areas of SDF. The limited records from within the central Brazilian Cerrado
460 show the expansion of gallery forests from ca. 3.5 – 3 ka (Silva et al., 2008), and in the
461 southernmost Brazilian Cerrado at ca. 1.5 ka (Behling et al., 2005). However, the paucity of
462 these sites means that it is uncertain whether this gallery forest expansion happened across
463 the Cerrado biome.
464
465 Across the southern Brazilian highlands, there is clear evidence of extensive areas of SAV
466 type vegetation (most likely campos grassland) from ca. 6 – 4 ka. An expansion of montane
467 forests along the coastal mountains of São Paulo and Rio de Janerio states occurred from
468 ca. 5 – 4 ka, and expansion of *Araucaria* forest on the southern Brazilian highlands occurred
469 from ca. 4 – 3.5 ka. Further expansion of *Araucaria* forests occurred within the last ca. 1.5 –
470 1 ka. The *Araucaria* forests were likely to have been particularly sensitive to even small
471 changes in the precipitation regime, as they currently grow where there is high annual
472 precipitation and a short, or ill-defined, dry season. The drier mid-Holocene climate and
473 associated expansion of campos grassland was probably linked with an increased dry
474 season length of around 3 months (Behling, 1997a; 1998; Behling and Pillar, 2007). The
475 initial phase of *Araucaria* expansion from ca. 4 – 3.5 ka was likely in the form of gallery
476 forests where moisture levels could be maintained more easily (Behling, 1997a; Behling et
477 al., 2004). The second phase of expansion from ca. 1.5 ka marks a more regional expanse
478 of *Araucaria* forest, suggesting that the precipitation regime was back to near-modern levels,

with high annual precipitation and a short, or ill-defined, dry season (Behling and Pillar, 2007). Again, these timings seem to match well with the Botuvera Cave paleoclimate records, which record increased tropical moisture source from ca. 4 ka, and a return to modern moisture levels from ca. 2 – 1.5 ka. The timings of *Araucaria* expansion also coincide with increasing human activity in the region, raising the possibility that humans could have taken advantage of a wetter climate and influenced the expansion of this economically useful taxon (Bitencourt and Krauspenhar, 2006; Iriarte and Behling, 2007; Iriarte et al., 2016).

Eastern Amazonia (EA)

A recently published speleothem record from Paraíso cave in eastern Amazonia suggests that this region may have been wetter than present at the mid Holocene (Wang et al., 2017), in contrast to other areas of the Amazon basin that record a drier mid-Holocene. The explanation for this pattern is still unclear; early-mid Holocene warming could have increased moisture supply, while weaker ENSO activity during the mid-Holocene may have reduced drought events in the eastern Amazon (Koutavas and Joanides, 2012; Wang et al., 2017), but these explanations do not necessarily account for the apparent wetter-than-present mid Holocene. Clearly, the robustness of, and potential mechanisms for, such a pattern requires more investigation. Vegetation reconstructions from most sites near to this speleothem record (e.g. site id's 1, 21-25) show stable HETF cover at the mid-Holocene (Behling and da Costa, 2001; Irion et al., 2006; Bush et al., 2007a), which is unsurprising if climate was wetter at this time.

This story is clearly a more complicated one if we consider the evidence of mid-to-late Holocene vegetation changes near to the south-eastern Amazonian ecotone, which appear to contradict Paraíso cave's mid-to-late Holocene precipitation history. A number of sites located on the Serra Sul dos Carajás plateau (ids = 30 – 32) indicate dominance of savannah and dry-adapted SDF arboreal taxa during the mid-Holocene (6 – 5 ka),

suggesting drier conditions, after which humid evergreen forest elements gradually increase up to ca. 4 – 3 ka, suggesting increasing moisture (Absy et al., 1991; Sifeddine et al., 2001; Hermanowski et al., 2014). Even though human occupation has been recorded in this region for at least the last 10 ka (Kipnis et al., 2005), the decrease in fire occurrences on the Carajás plateau that are recorded during the mid-Holocene at Lagoa de Cachoeira (id = 31) would suggest that the more open vegetation at this time was not initiated by human land management. In fact, a more likely scenario is the abandonment of the plateau by humans at this time (so fewer anthropogenic fires) due to a reduction in both water sources and forest resources (Hermanowski et al., 2014). Therefore, the apparent mismatch between these vegetation changes and the climate change at Paraíso Cave is unlikely to be due to human impacts. Around 175 km north-east of the Carajás plateau, the Lake Marabá record (id = 29) indicates a switch to a HETF dominated signal at ca. 5 ka (Guimarães et al., 2013a).

Some important considerations must be noted with regards to these records that seem to contradict the regional paleoclimate history. There is clearly a paucity of paleoecological sites across this south-eastern Amazonian ecotonal area, so it is difficult to infer any regional scale vegetation changes. Furthermore, the sites we do have are predominantly located on the Serra Sul dos Carajás plateau. It has long been debated as to how well the HETF surrounding the plateau is represented in the plateau based pollen records (Absy et al., 1991; 2014; Guimarães et al., 2014). The consensus at this time is that the plateau vegetation, along with some input from the forests growing on the slopes, dominates the pollen assemblages of the lake and bog records from the plateau, suggesting that the mid-to-late Holocene Carajás records only reflect local changes on the plateau itself (Hermanowski et al., 2012a; 2012b; 2014). At the nearby Lake Marabá record, the vegetation changes could be due to successional vegetation changes after the formation of the lake (Guimarães et al., 2013a). Even given these caveats, there is still a mismatch between vegetation reconstructions apparently indicating a drier mid-Holocene (at a local

scale) and the Paraíso cave record indicating a wetter regional climate. Clearly more work needs to be done to reconcile these differences.

North-Eastern Brazil (NE)

As the modern east-west precipitation dipole between north-eastern Brazil (dry climate) and the central South American tropics (wet climate) is largely controlled by the strength of the SASM and associated features, it is not unexpected to find that the paleoprecipitation history of the Rio Grande do Norte speleothem shows a distinct 'anti-phased' relationship to the rest of tropical South America (Cruz et al., 2009; Cheng et al., 2013). During the mid-Holocene, when insolation levels were low and the south and west SASM region was drier, the nordeste was wetter than at present (Fig 3h). Mechanistically, this is most likely due to a weaker SASH and weaker convective activity in the core of the SASM region reducing the strength of the nordeste low and subsidence over the region (Cruz et al., 2009; Cheng et al., 2013). Weaker ENSO activity during the mid-Holocene may also have reduced severe drought events in this region (Koutavas and Joanides, 2012; Wang et al., 2017). As insolation levels increase through the Holocene, the region becomes gradually drier, reaching approximately modern levels at ca. 4 ka. Reconstructing the paleovegetation history of this region in response to this sort of long-term precipitation change is of great interest, for example in terms of revealing important information about the potential connectivity between the Amazon and Atlantic rainforests (De Oliveira et al., 1999; Behling et al., 2000; Costa, 2003; Batalha-Filho et al., 2013). However, a fundamental issue in this semi-arid region is the difficulty in finding permanent lake basins, bogs, or undisturbed locations for taking soil profiles, that would provide suitable records for paleoecological study (De Oliveira et al., 1999; Pessenda et al., 2010).

The pollen record from the site Saquinho (id = 34), taken in the Caatinga region in the Rio Icatu river valley, suggests that a more humid mid-Holocene may have promoted the expansion of palms and gallery forests at the expense of Caatinga/savannah vegetation.

Between ca. 5 and 4.5 ka, the trend of increasing aridity in the region is marked by an increase in Caatinga and Cerrado taxa as well as a reactivation of dune activity shown by thermoluminescence data (De Oliveira et al., 1999). The Maranguape bog core taken from the Serra de Maranguape mountains on the north coast (id = 28) records continuous forest cover through the mid-to-late Holocene, though compositional changes in the pollen record suggest increased disturbance at ca. 4.5 ka, contemporaneous with the start of drier conditions in the nordeste (Montade et al., 2014). However, other records in this region do not seem to reflect the more humid mid-Holocene in their paleovegetation reconstructions, though this is most likely due to the unique characteristics of their site locations. A transect of soil profiles on the Araripe Plateau in the central Caatinga region (ids = 78 – 80) records gradual depletion of $\delta^{13}C$ from the mid-Holocene to present, suggesting greater savannah extent before ca. 3.5 – 3 ka, after which forested areas increase. A transect of soil profiles on the east coast of Paraíba state (ids = 76 – 77) also show some indications of more open vegetation in the mid-Holocene, with an increase in forest cover after ca. 3 ka. The modern rainforest enclaves on plateaus such as Araripe and on higher elevations near the coast are maintained by significant orographic rainfall derived from easterly winds that help to mitigate against the arid conditions caused by the persistent subsidence (Andrade-Lima, 1982; Sampaio, 1995). Even though this subsidence was likely reduced during the mid-Holocene causing the region in general to become less arid, changes to low-level divergent circulation patterns and Walker cell dynamics may also have reduced the moist easterlies (Cruz et al., 2009) that helps maintain these plateau-based forests. Whilst these small plateaus and coastal areas can yield suitable sites, clearly they may not be representative of vegetation changes across the Caatinga on a regional scale. The site of Lagoa do Caçó (id = 11) is located on the northernmost reach of the Cerrado savannah biome and records no major changes in the Cerrado vegetation through the mid-to-late Holocene (Ledru et al., 2006). The increase in gallery forests around the lake shown in the nearby soil pits may indicate increased moisture after ca. 4 ka, though it is difficult to say whether this is due to climate, natural vegetation succession or sea level dynamics. The authors suggest that the location

591 of this lake lies in a transitional area between the east-west climate zones and as such,
592 precipitation changes may be fairly stable in contrast to the surrounding areas (Pessenda et
593 al., 2005; Ledru et al., 2006).

CONCLUSIONS

Our multi-proxy paleoecological data synthesis shows how the vegetation from different regions of tropical South America responded to orbitally forced long-term precipitation changes through the mid-to-late Holocene (Cheng et al., 2013; Baker and Fritz, 2015). The HETF biome of central and western Amazonia remained intact, even though paleoclimate records suggest that this region may have been slightly drier than present during the mid-Holocene. In eastern Amazonia, similar HETF stability is recorded, however the apparent mid-Holocene savannah expansion at the eastern Amazonian ecotone (from the Serra Sul dos Carajás plateau) is difficult to reconcile with new paleoclimate data from Paraíso cave that suggests this region was wetter than present at this time (Wang et al., 2017). The Paraíso cave record perhaps only reflects precipitation conditions from far north-east Amazonia, and is not representative of Carajás' location in south-east Amazonia. Nearer to the south-eastern Amazonian ecotone and the Carajás plateau, local lake level records appear to indicate lower lake productivity and water levels during the mid-Holocene, indicative of a drier climate (Cordeiro et al., 2008). Clearly more investigation is needed in this area to reconcile local and regional paleoclimate and paleoecological records. The north-east of Brazil was wetter than present during the mid Holocene, due to a suppression of the subsidence across the region resulting from a weaker SASM and SASH (Cruz et al., 2009). However, the lack of paleovegetation records means a regional interpretation of vegetation response is problematic.

Significant vegetation changes are recorded in south-west Amazonia and south-east Brazil. These regions are more reliant on SASM-derived precipitation and so vegetation here is likely to be especially susceptible to long-term changes in SASM strength. The vegetation reconstructions during a drier mid-Holocene show: a more northerly location of the HETF/SDF/SAV ecotone in north-eastern Bolivia; greater expanse of campos grassland across the south Brazilian highlands; and decreased expanse of montane forests and HETF across the southern Atlantic forest region. As precipitation levels gradually rose through the

622 mid-to-late Holocene, vegetation responded as follows: progressive southward expansion of
623 the HETF in north-east Bolivia from ca. 2 ka; expansion of Araucaria on the south Brazilian
624 highlands from ca. 4 ka, with enhanced expansion from ca. 1.5 – 1 ka; expansion, or greater
625 canopy density, of SDF in the Misiones and interior Atlantic forest regions; increase of
626 gallery forests in the south-east Brazilian Cerrado. The difference in the timing of forest
627 expansion between these two regions is probably due to the important extra-tropical source
628 of precipitation that mitigates somewhat against a weaker SASM in south-east Brazil.
629
630 Whilst this synthesis includes more sites than previous studies, in part due to inclusion of
631 non-pollen proxy reconstructions, it is clear that more sites are needed to help increase our
632 understanding of long-term vegetation dynamics across the region. In south-west Amazonia,
633 more sites could help to quantify the maximum extent of the HETF/SDF/savannah mid-to-
634 late Holocene ecotonal shift. We particularly highlight eastern Amazonia, north-east Brazil
635 and the cerrado region of central Brazil as key areas that need more paleoecological data.
636 We recognise that the paucity of suitable lake sites in these areas is a big hindrance to
637 improving the regional coverage of pollen-based vegetation reconstructions. However, in
638 such regions, where suitable lakes/bogs are scarce, soil-based proxies – such as $\delta^{13}C$
639 isotopes and, in particular, phytoliths – which have hitherto been underutilised by the
640 paleoecological community, show considerable potential for paleovegetation reconstruction
641 (Dickau et al., 2013; Watling et al., 2016; 2017).
642
643 With regards to possible implications for future climate change, this study highlights that the
644 ecosystems most vulnerable to long-term climate change are those that are already close to
645 their climatic limits. However, given the resilience of the central Amazonian HETF biome to
646 past climate change, future projections of widespread forest dieback across Amazonia (Cox
647 et al., 2000; 2004) seem unlikely. It is important to point out that we have used the mid-to-
648 late Holocene as a period in which we can assess regional vulnerability to long-term climate
649 changes, not as a direct analogue for a future drier climate. Factors such as temperature

and CO_2 levels will be significantly different between the future and the mid-Holocene, which will undoubtedly have an impact on vegetation responses (Rammig et al., 2010; Huntingford et al., 2013). In addition, huge anthropogenic pressures, such as widespread deforestation and uncontrolled burning, will only act to reduce the ability of vegetation to maintain local feedbacks and thus reduce overall ecosystem resilience (Laurance et al., 2000; Malhi et al., 2008; Levine et al., 2016).

ACKNOWLEDGEMENTS

We thank Francisco Cruz and Bronwen Whitney, who provided paleoclimate data for Rio Grande do Norte and Laguna La Gaiba, respectively. Other speleothem data and insolation data were accessed online via the National Oceanic and Atmospheric Administration (NOAA) website: https://www.ncdc.noaa.gov/paleo. Tropical Rainfall Measuring Mission (TRMM) data (https://trmm.gsfc.nasa.gov) were processed by the TRMM Science Data and Information System (TSDIS) and the TRMM office and are archived and distributed by the Goddard Distributed Active Archive Center. RS was funded by a NERC 'SCENARIO' DTP PhD award**.** We thank Mark Bush for the invitation to submit a paper to this special issue of QR and are grateful for his comments, and those of two referees, which improved the manuscript.

668 **LIST OF TABLES**

669 **Table 1.** List of paleoecological sites. 'ID' number refers to location number in Fig. 2a. Size
670 categories refer to those outlined in Table 3. Subscript numbers next to site names refer to
671 the proxy types used in that study: 1 = pollen analysis; 2 = charcoal analysis; 3 = isotopic
672 analysis; 4 = physio-chemical analysis. Asterisk next to site ID indicates a site where an
673 independent age-depth model was created (see methods).

674

675 **Table 2.** Description of the broad vegetation classifications used in this study

676

677 **Table 3.** Size categories representing the different catchment areas of the paleoecological
678 sites

679 **LIST OF FIGURES**

680 **Figure 1.** Observed long-term mean precipitation (mm/day), 850 mb wind speed and wind
681 direction for (a) June, July and August (JJA), and (b) December, January, February (DJF).
682 Labels indicate key climate features: Intertropical Convergence Zone (ITCZ), South
683 American Low Level Jet (SALLJ), Chaco Low (CL), South Atlantic Convergence Zone
684 (SACZ), South Atlantic Subtropical High (SASH), and Nordeste Low (NL) - see text for
685 details. Precipitation data taken from Tropical Rainfall Measuring Mission v7 (TRMM) 3B43
686 dataset (1998-2014) (Huffman et al., 2007). Wind data taken from NCEP Climate Forecast
687 System Reanalysis (CFSR) dataset (1979-2010) (Saha et al., 2010a; 2010b).
688
689 **Figure 2.** Overview maps of study area, (a) location and numeric ID of each site
690 corresponding to Table 1, (b) broad modern vegetation biomes, modified from Olson et al.
691 (2001), (c) long term average annual precipitation based on Tropical Rainfall Measuring
692 Mission v7 (TRMM) 3B43 dataset (1998-2014) (Huffman et al., 2007). The polygons shown
693 in (b) and (c) represent the regions discussed in text: CW = Central and western lowland
694 Amazonia, EA = Eastern Amazonia, SW = South-Western Amazonia, SB = South-eastern
695 Brazil, NE = North-eastern Brazil. The blue squares in (b) and (c) show locations of the
696 paleoclimate sites discussed in text: 1 = El Condor, 2 = Cueva del Tigre Perdido, 3 = Lake
697 Junin, 4 = Huaguapo, 5 = Lake Titicaca, 6 = Laguna La Gaiba, 7 = Botuvera Cave, 8 = Rio
698 Grande do Norte, 9 = Paraíso Cave
699
700 **Figure 3.** Selected paleoclimate records representing proxy records for precipitation
701 changes through the last 6 ka, shown alongside calculated January insolation at 15°S
702 (Berger and Loutre, 1991; Berger, 1992) (a) $\delta^{18}O$ of stalagmite Core A and Core B from El
703 Condor Cave (Cheng et al., 2013), (b) $\delta^{18}O$ of stalagmite records NC-A and NC-B from
704 Cueva del Tigre Perdido (van Breukelen et al., 2008), (c) $\delta^{18}O$ of calcite from Lake Junin
705 (Seltzer et al., 2000), (d) $\delta^{18}O$ of speleothem record Huaguapo (Kanner et al., 2013), (e)

706 lake-level changes as measured by $\delta^{13}C$ at Lake Titicaca (Rowe et al., 2002), (f)
707 *Pediastrum*-inferred lake-level change at Laguna La Gaiba (Whitney and Mayle, 2012), (g)
708 $\delta^{18}O$ of speleothem record BTV3a, Sr/Ca of speleothem BTV21a from Botuvera Cave (BTV)
709 site (Wang et al., 2007; Bernal et al., 2016), (h) $\delta^{18}O$ of speleothem records FN1, RN1 and
710 RN4 from the Rio Grande do Norte (RGDN) record (Cruz et al., 2009).
711
712 **Figure 4.** Paleoecological reconstructions at 0.5 ka time slices from 6 ka to present.
713 Background of modern vegetation biomes, modified from Olson et al. (2001). Vegetation
714 classifications outlined in Table 2. Size of circles represents catchment area of that site,
715 outlined in Table 3.

REFERENCES

Absy, M.L., Cleef, A., Fournier, M., Martin, L., Servant, M., Sifeddine, A., Ferreira da Silva, M., Soubiès, F., Suguio, K., Turcq, B., van der Hammen, T., 1991. Mise en évidence de quatre phases d'ouverture de la forêt dense dans le Sud-Est de l'Amazonie au cours des 60 000 dernières années: première comparaison avec d'autres régions tropicales. Comptes rendus de l"Académie des sciences. Série 2, Mécanique, Physique, Chimie, Sciences de l"univers, Sciences de la Terre 312, 673–678.

Absy, M.L., Cleef, A.M., D'Apolito, C., da Silva, M.F.F., 2014. Palynological differentiation of savanna types in Carajás, Brazil (southeastern Amazonia). Palynology 38, 78–89.

Adeney, J.M., Christensen, N.L., Vicentini, A., Cohn-Haft, M., 2016. White-sand Ecosystems in Amazonia. Biotropica 48, 7–23.

Alexandre, A., Meunier, J.D., Mariotti, A., Soubiès, F., 1999. Late Holocene phytolith and carbon-isotope record from a latosol at Salitre, south-central Brazil. Quaternary Research 51, 187–194.

Andrade-Lima, D. de, 1982. Present-day forest refuges in northeastern Brazil. In: Biological Diversification in the Tropics. Columbia University Press, New York, pp. 245–251.

Baker, P.A., Fritz, S.C., 2015. Nature and causes of Quaternary climate variation of tropical South America. Quaternary Science Reviews 124, 31–47.

Baker, P.A., Seltzer, G.O., Fritz, S.C., Dunbar, R.B., Grove, M.J., Tapia, P.M., Cross, S.L., Rowe, H.D., Broda, J.P., 2001. The history of South American tropical precipitation for the past 25,000 years. Science 291, 640–643.

Barberi, M., Salgado-Labouriau, M.L., Suguio, K., 2000. Paleovegetation and paleoclimate of "Vereda de Águas Emendadas," central Brazil. Journal of South American Earth Sciences 13, 241–254.

740 Batalha-Filho, H., Fjeldså, J., Fabre, P.H., Miyaki, C.Y., 2013. Connections between the
741 Atlantic and the Amazonian forest avifaunas represent distinct historical events. Journal
742 of Ornithology 154, 41–50.

743 Behling, H., 1995a. A high resolution Holocene pollen record from Lago do Pires, SE Brazil:
744 vegetation, climate and fire history. Journal of Paleolimnology 14, 253–268.

745 Behling, H., 1995b. Investigations into the late Pleistocene and Holocene history of
746 vegetation and climate in Santa Catarina (S Brazil). Vegetation History and
747 Archaeobotany 4, 127–152.

748 Behling, H., 1997a. Late Quaternary vegetation, climate and fire history of the Araucaria
749 forest and campos region from Serra Campos Gerais, Paraná State (South Brazil).
750 Review of Palaeobotany and Palynology 97, 109–121.

751 Behling, H., 1997b. Late Quaternary vegetation, climate and fire history from the tropical
752 mountain region of Morro de Itapeva, SE Brazil. Palaeogeography, Palaeoclimatology,
753 Palaeoecology 129, 407–422.

754 Behling, H., 1998. Late Quaternary vegetational and climatic changes in Brazil. Review of
755 Palaeobotany and Palynology 99, 143–156.

756 Behling, H., 2003. Late glacial and Holocene vegetation, climate and fire history inferred
757 from Lagoa Nova in the southeastern Brazilian lowland. Vegetation History and
758 Archaeobotany 12, 263–270.

759 Behling, H., 2007. Late Quaternary vegetation, fire and climate dynamics of Serra do
760 Araçatuba in the Atlantic coastal mountains of Paraná State, southern Brazil. Vegetation
761 History and Archaeobotany 16, 77–85.

762 Behling, H., Arz, H.W., Pätzold, J., Wefer, G., 2000. Late Quaternary vegetational and
763 climate dynamics in northeastern Brazil, inferences from marine core GeoB 3104-1.

764 Quaternary Science Reviews 19, 981–994.

765 Behling, H., Bauermann, S.G., Pereira Neves, P.C., 2001a. Holocene environmental
766 changes in the São Francisco de Paula region, southern Brazil. Journal of South
767 American Earth Sciences 14, 631–639.

768 Behling, H., Berrio, J.C., Hooghiemstra, H., 1999. Late Quaternary pollen records from the
769 middle Caquetá river basin in central Colombian Amazon. Palaeogeography,
770 Palaeoclimatology, Palaeoecology 145, 193–213.

771 Behling, H., Cohen, M.C.L., Lara, R.J., 2001b. Studies on Holocene mangrove ecosystem
772 dynamics of the Bragança Peninsula in north-eastern Pará, Brazil. Palaeogeography,
773 Palaeoclimatology, Palaeoecology 167, 225–242.

774 Behling, H., da Costa, M.L., 2000. Holocene Environmental Changes from the Rio Curuá
775 Record in the Caxiuanã Region, Eastern Amazon Basin. Quaternary Research 53, 369–
776 377.

777 Behling, H., da Costa, M.L., 2001. Holocene vegetational and coastal environmental
778 changes from the Lago Crispim record in northeastern Pará State, eastern Amazonia.
779 Review of Palaeobotany and Palynology 114, 145–155.

780 Behling, H., Dupont, L., Safford, H.D., Wefer, G., 2007. Late Quaternary vegetation and
781 climate dynamics in the Serra da Bocaina, southeastern Brazil. Quaternary International
782 161, 22–31.

783 Behling, H., Keim, G., Irion, G., Junk, W., Nunes de Mello, J., 2001c. Holocene
784 environmental changes in the Central Amazon Basin inferred from Lago Calado (Brazil).
785 Palaeogeography, Palaeoclimatology, Palaeoecology 173, 87–101.

786 Behling, H., Negrelle, R.R.B., 2001. Tropical Rain Forest and Climate Dynamics of the
787 Atlantic Lowland, Southern Brazil, during the Late Quaternary. Quaternary Research 56,

383–389.

Behling, H., Negrelle, R.R.B., Colinvaux, P.A., 1997. Modern pollen rain data from the tropical Atlantic rain forest, Reserva Volta Velha, South Brazil. Review of Palaeobotany and Palynology 97, 287–299.

Behling, H., Pillar, V.D., 2007. Late Quaternary vegetation, biodiversity and fire dynamics on the southern Brazilian highland and their implication for conservation and management of modern Araucaria forest and grassland ecosystems. Philosophical Transactions of the Royal Society B: Biological Sciences 362, 243–251.

Behling, H., Pillar, V.D., Bauermann, S.G., 2005. Late Quaternary grassland (Campos), gallery forest, fire and climate dynamics, studied by pollen, charcoal and multivariate analysis of the São Francisco de Assis core in western Rio Grande do Sul (southern Brazil). Review of Palaeobotany and Palynology 133, 235–248.

Behling, H., Pillar, V.D., Orlóci, L., Bauermann, S.G., 2004. Late Quaternary Araucaria forest, grassland (Campos), fire and climate dynamics, studied by high-resolution pollen, charcoal and multivariate analysis of the Cambará do Sul core in southern Brazil. Palaeogeography, Palaeoclimatology, Palaeoecology 203, 277–297.

Behling, H., Safford, H.D., 2010. Late- glacial and Holocene vegetation, climate and fire dynamics in the Serra dos Órgãos, Rio de Janeiro State, southeastern Brazil. Global Change Biology 16, 1661–1671.

Berger, A., 1992. Orbital Variations and Insolation Database. IGBP PAGES/World Data Center-A for Paleoclimatology Data Contribution Series #92-007. NOAA/NGDC Paleoclimatology Program, Boulder CO, USA.

Berger, A., Loutre, M.F., 1991. Insolation values for the climate of the last 10 million years. Quaternary Science Reviews 10, 297–317.

812 Bernal, J.P., Cruz, F.W., Stríkis, N.M., Wang, X., Deininger, M., Catunda, M.C.A., Ortega-
813 Obregón, C., Cheng, H., Edwards, R.L., Auler, A.S., 2016. High-resolution Holocene
814 South American monsoon history recorded by a speleothem from Botuverá Cave, Brazil.
815 Earth and Planetary Science Letters 450, 186–196.

816 Bitencourt, A., Krauspenhar, P.M., 2006. Possible prehistoric anthropogenic effect on
817 Araucaria angustifolia (Bert.) O. Kuntze expansion during the Late Holocene. Revista
818 Brasileira de Paleontologia 9, 109–116.

819 Blaauw, M., Christen, J.A., 2011. Flexible paleoclimate age-depth models using an
820 autoregressive gamma process. Bayesian Analysis 6, 457–474.

821 Boisier, J.P., Ciais, P., Ducharne, A., Guimberteau, M., 2015. Projected strengthening of
822 Amazonian dry season by constrained climate model simulations. Nature Climate
823 Change 5, 656–660.

824 Boutton, T.W., 1996. Stable carbon isotopes ratios of soil organic matter and their use of
825 indicators of vegetation and climate change. In: Boutton, T.W., Yamasaki, S. (Eds.),
826 Mass Spectrometry of Soils. New York, pp. 47–82.

827 Braconnot, P., Harrison, S.P., Otto-Bliesner, B., Abe-Ouchi, A., Jungclaus, J., Peterschmitt,
828 J.Y., 2011. The Paleoclimate Modeling Intercomparison Project contribution to CMIP5.
829 CLIVAR Exchanges 16, 15–19.

830 Brugger, S.O., Gobet, E., van Leeuwen, J.F.N., Ledru, M.-P., Colombaroli, D., van der
831 Knaap, W.O., Lombardo, U., Escobar-Torrez, K., Finsinger, W., Rodrigues, L., Giesche,
832 A., Zarate, M., Veit, H., Tinner, W., 2016. Long-term man-environment interactions in the
833 Bolivian Amazon: 8000 years of vegetation dynamics. Quaternary Science Reviews 132,
834 114–128.

835 Burbridge, R.E., Mayle, F.E., Killeen, T.J., 2004. Fifty-thousand-year vegetation and climate

history of Noel Kempff Mercado National Park, Bolivian Amazon. Quaternary Research 61, 215–230.

Bush, M.B., Colinvaux, P.A., 1988. A 7000-Year Pollen Record from the Amazon Lowlands, Ecuador. Vegetatio 76, 141–154.

Bush, M.B., Correa-Metrio, A., McMichael, C.N.H., Sully, S., Shadik, C.R., Valencia, B.G., Guilderson, T., Steinitz-Kannan, M., Overpeck, J.T., 2016. A 6900-year history of landscape modification by humans in lowland Amazonia. Quaternary Science Reviews 141, 52–64.

Bush, M.B., De Oliveira, P.E., Colinvaux, P.A., Miller, M.C., Moreno, J.E., 2004a. Amazonian paleoecological histories: one hill, three watersheds. Palaeogeography, Palaeoclimatology, Palaeoecology 214, 359–393.

Bush, M.B., Miller, M.C., De Oliveira, P.E., Colinvaux, P.A., 2000. Two histories of environmental change and human disturbance in eastern lowland Amazonia. The Holocene 10, 543–553.

Bush, M.B., Rivera, R., 2001. Reproductive ecology and pollen representation among neotropical trees. Global Ecology and Biogeography 10, 359–367.

Bush, M.B., Silman, M.R., De Toledo, M.B., Listopad, C., Gosling, W.D., Williams, C., De Oliveira, P.E., Krisel, C., 2007a. Holocene fire and occupation in Amazonia: records from two lake districts. Philosophical Transactions of the Royal Society B: Biological Sciences 362, 209–218.

Bush, M.B., Silman, M.R., Listopad, C.M.C.S., 2007b. A regional study of Holocene climate change and human occupation in Peruvian Amazonia. Journal of Biogeography 34, 1342–1356.

Bush, M.B., Silman, M.R., Urrego, D.H., 2004b. 48,000 years of climate and forest change in

a biodiversity hot spot. Science 303, 827–829.

Calegari, M.R., Madella, M., Vidal-Torrado, P., Pessenda, L.C.R., Marques, F.A., 2013. Combining phytoliths and δ13C matter in Holocene palaeoenvironmental studies of tropical soils: An example of an Oxisol in Brazil. Quaternary International 287, 47–55.

Carson, J.F., Mayle, F.E., Whitney, B.S., Iriarte, J., Soto, J.D., 2016. Pre-Columbian ring ditch construction and land use on a “chocolate forest island” in the Bolivian Amazon. Journal of Quaternary Science 31, 337–347.

Carson, J.F., Watling, J., Mayle, F.E., Whitney, B.S., Iriarte, J., Prümers, H., Soto, J.D., 2015. Pre-Columbian land use in the ring-ditch region of the Bolivian Amazon. The Holocene 25, 1285–1300.

Carson, J.F., Whitney, B.S., Mayle, F.E., Iriarte, J., Prümers, H., Soto, J.D., Watling, J., 2014. Environmental impact of geometric earthwork construction in pre-Columbian Amazonia. Proceedings of the National Academy of Sciences 111, 10497–10502.

Carvalho, L., Jones, C., Liebmann, B., 2004. The South Atlantic convergence zone: Intensity, form, persistence, and relationships with intraseasonal to interannual activity and extreme rainfall. Journal of Climate 17, 88–108.

Cassino, R.F., Meyer, K.E.B., 2013. Reconstituição paleoambiental do Chapadão dos Gerais (Quaternário tardio) a partir da análise palinológica da Vereda Laçador, Minas Gerais, Brasil. Revista Brasileira de Paleontologia 16, 127–146.

Chen, T.-C., Weng, S.-P., Schubert, S., 1999. Maintenance of Austral Summertime Upper-Tropospheric Circulation over Tropical South America: The Bolivian High–Nordeste Low System. Journal of the Atmospheric Sciences 56, 2081–2100.

Cheng, H., Sinha, A., Cruz, F.W., Wang, X., Edwards, R.L., d'Horta, F.M., Ribas, C.C., Vuille, M., Stott, L.D., Auler, A.S., 2013. Climate change patterns in Amazonia and

884 biodiversity. Nature communications 4, 1411.

885 Cohen, M.C.L., Rossetti, D. de F., Pessenda, L.C.R., Friaes, Y.S., Oliveira, P.E., 2014. Late
886 Pleistocene glacial forest of Humaitá—Western Amazonia. Palaeogeography,
887 Palaeoclimatology, Palaeoecology 415, 37–47.

888 Colinvaux, P.A., De Oliveira, P.E., Moreno, J.E., Miller, M.C., 1996. A long pollen record
889 from lowland Amazonia: forest and cooling in glacial times. Science 274, 85–88.

890 Cordeiro, R.C., Turcq, B., Suguio, K., Oliveira da Silva, A., Sifeddine, A., Volkmer-Ribeiro,
891 C., 2008. Holocene fires in East Amazonia (Carajás), new evidences, chronology and
892 relation with paleoclimate. Global and Planetary Change 61, 49–62.

893 Costa, L.P., 2003. The historical bridge between the Amazon and the Atlantic Forest of
894 Brazil: a study of molecular phylogeography with small mammals. Journal of
895 Biogeography 30, 71–86.

896 Cowling, S.A., Shin, Y., 2006. Simulated ecosystem threshold responses to co-varying
897 temperature, precipitation and atmospheric CO2 within a region of Amazonia. Global
898 Ecology and Biogeography 15, 553–566.

899 Cox, P.M., Betts, R.A., Collins, M., Harris, P.P., Huntingford, C., Jones, C.D., 2004.
900 Amazonian forest dieback under climate-carbon cycle projections for the 21st century.
901 Theoretical and Applied Climatology 78.

902 Cox, P.M., Betts, R.A., Jones, C.D., Spall, S.A., Totterdell, I.J., 2000. Acceleration of global
903 warming due to carbon-cycle feedbacks in a coupled climate model. Nature 408, 184–
904 187.

905 Cruz, F.W., Burns, S.J., Karmann, I., Sharp, W.D., Vuille, M., Cardoso, A.O., Ferrari, J.A.,
906 Dias, P.L.S., Viana, O., 2005. Insolation-driven changes in atmospheric circulation over
907 the past 116,000 years in subtropical Brazil. Nature 434, 63–66.

908 Cruz, F.W., Burns, S.J., Karmann, I., Sharp, W.D., Vuille, M., Ferrari, J.A., 2006. A
909 stalagmite record of changes in atmospheric circulation and soil processes in the
910 Brazilian subtropics during the Late Pleistocene. Quaternary Science Reviews 25,
911 2749–2761.

912 Cruz, F.W., Vuille, M., Burns, S.J., Wang, X., Cheng, H., Werner, M., Edwards, R.L.,
913 Karmann, I., Auler, A.S., Nguyen, H., 2009. Orbitally driven east-west antiphasing of
914 South American precipitation. Nature Geoscience 2, 210–214.

915 Davis, M.B., 2000. Palynology after Y2K - Understanding the source area of pollen in
916 sediments. Annual Review of Earth and Planetary Sciences 28, 1–18.

917 de Freitas, H.A., Pessenda, L.C.R., Aravena, R., Gouveia, S.E.M., de Souza Ribeiro, A.,
918 Boulet, R., 2001. Late Quaternary Vegetation Dynamics in the Southern Amazon Basin
919 Inferred from Carbon Isotopes in Soil Organic Matter. Quaternary Research 55, 39–46.

920 De Oliveira, P.E., Barreto, A.M.F., Suguio, K., 1999. Late Pleistocene/Holocene climatic and
921 vegetational history of the Brazilian caatinga: the fossil dunes of the middle São
922 Francisco River. Palaeogeography, Palaeoclimatology, Palaeoecology 152, 319–337.

923 Dickau, R., Whitney, B.S., Iriarte, J., Mayle, F.E., Soto, J.D., Metcalfe, P., Street-Perrott,
924 F.A., Loader, N.J., Ficken, K.J., Killeen, T.J., 2013. Differentiation of neotropical
925 ecosystems by modern soil phytolith assemblages and its implications for
926 palaeoenvironmental and archaeological reconstructions. Review of Palaeobotany and
927 Palynology 193, 1–23.

928 Doughty, C.E., Metcalfe, D.B., Girardin, C.A.J., Amézquita, F.F., Cabrera, D.G., Huasco,
929 W.H., Silva-Espejo, J.E., Araujo-Murakami, A., da Costa, M.C., Rocha, W., Feldpausch,
930 T.R., Mendoza, A.L.M., da Costa, A.C.L., Meir, P., Phillips, O.L., Malhi, Y., 2015.
931 Drought impact on forest carbon dynamics and fluxes in Amazonia. Nature 519, 78–82.

Duffy, P.B., Brando, P.M., Asner, G.P., Field, C.B., 2015. Projections of future meteorological drought and wet periods in the Amazon. Proceedings of the National Academy of Sciences 112, 13172–13177.

Dümig, A., Schad, P., Rumpel, C., Dignac, M.-F., Kögel-Knabner, I., 2008. Araucaria forest expansion on grassland in the southern Brazilian highlands as revealed by 14C and δ13C studies. Geoderma 145, 143–157.

Eltahir, E., Bras, R.L., 1994. Precipitation recycling in the Amazon basin. Quaternary Journal of the Royal Meteorological Society 120, 861–880.

Enters, D., Behling, H., Mayr, C., Dupont, L., Zolitschka, B., 2010. Holocene environmental dynamics of south-eastern Brazil recorded in laminated sediments of Lago Aleixo. Journal of Paleolimnology 44, 265–277.

Feldpausch, T.R., Phillips, O.L., Brienen, R.J.W., Gloor, E., Lloyd, J., Lopez-Gonzalez, G., Monteagudo-Mendoza, A., Malhi, Y., Alarcón, A., Dávila, E.Á., Alvarez-Loayza, P., Andrade, A.S., Aragão, L.E.O.C., Arroyo, L., C, G.A.A., Baker, T.R., Baraloto, C., Barroso, J., Bonal, D., Castro, W., Chama, V., Chave, J., Domingues, T.F., Fauset, S., Groot, N., Coronado, E.H., Laurance, S.G.W., Laurance, W.F., Lewis, S.L., Licona, J.C., Marimon, B.S., Marimon-Junior, B.H., Bautista, C.M., Neill, D.A., Oliveira, E.A., Santos, dos, C.O., Camacho, N.C.P., Pardo-Molina, G., Prieto, A., Quesada, C.A., Ramírez, F., Ramirez-Angulo, H., Réjou-Méchain, M., Rudas, A., Saiz, G., Salomao, R.P., Silva-Espejo, J.E., Silveira, M., Steege, ter, H., Stropp, J., Terborgh, J., Thomas-Caesar, R., van der Heijden, G.M.F., Martínez, R.V., Vilanova, E., Vos, V., 2016. Amazon forest response to repeated droughts. Biogeosciences 30, 964–982.

Flantua, S.G.A., Hooghiemstra, H., Grimm, E.C., Behling, H., Bush, M.B., González-Arango, C., Gosling, W.D., Ledru, M.-P., Lozano-García, S., Maldonado, A., Prieto, A.R., Rull, V., Van Boxel, J.H., 2015. Updated site compilation of the Latin American Pollen Database.

957 Review of Palaeobotany and Palynology 223, 104–115.

958 Flantua, S.G.A., Hooghiemstra, H., Vuille, M., Behling, H., Carson, J.F., Gosling, W.D.,
959 Hoyos, I., Ledru, M.-P., Montoya, E., Mayle, F.E., Maldonado, A., Rull, V., Tonello, M.S.,
960 Whitney, B.S., González-Arango, C., 2016. Climate variability and human impact in
961 South America during the last 2000 years: synthesis and perspectives from pollen
962 records. 12, 483–523.

963 Garreaud, R.D., Vuille, M., Compagnucci, R., Marengo, J.A., 2009. Present-day South
964 American climate. Palaeogeography, Palaeoclimatology, Palaeoecology 281, 180–195.

965 Gentry, A.H., 1995. Diversity and floristic composition of neotropical dry forests. In: Bullock,
966 S.H., Mooney, H.A., Medina, E. (Eds.), Seasonally Dry Tropical Forests. Cambridge
967 University Press, Cambridge, United Kingdom, pp. 146–194.

968 Gosling, W.D., Mayle, F.E., Tate, N.J., Killeen, T.J., 2005. Modern pollen-rain characteristics
969 of tall terra firme moist evergreen forest, southern Amazonia. Quaternary Research 64,
970 284–297.

971 Gosling, W.D., Mayle, F.E., Tate, N.J., Killeen, T.J., 2009. Differentiation between
972 Neotropical rainforest, dry forest, and savannah ecosystems by their modern pollen
973 spectra and implications for the fossil pollen record. Review of Palaeobotany and
974 Palynology 153, 70–85.

975 Gouveia, S.E.M., Pessenda, L.C.R., Aravena, R., Boulet, R., Scheel-Ybert, R., Bendassolli,
976 J.A., Ribeiro, A.S., de Freitas, H.A., 2002. Carbon isotopes in charcoal and soils in
977 studies of paleovegetation and climate changes during the late Pleistocene and the
978 Holocene in the southeast and centerwest regions of Brazil. Global and Planetary
979 Change 33, 95–106.

980 Guimarães, J.T.F., Cohen, M.C.L., França, M.C., Alves, I.C.C., Smith, C.B., Pessenda,

L.C.R., Behling, H., 2013a. An integrated approach to relate Holocene climatic, hydrological, morphological and vegetation changes in the southeastern Amazon region. Vegetation History and Archaeobotany 22, 185–198.

Guimarães, J.T.F., Cohen, M.C.L., França, M.C., Pessenda, L.C.R., Behling, H., 2013b. Morphological and vegetation changes on tidal flats of the Amazon Coast during the last 5000 cal. yr BP. The Holocene 23, 528–543.

Guimarães, J.T.F., Cohen, M.C.L., Pessenda, L.C.R., França, M.C., Smith, C.B., Nogueira, A.C.R., 2012. Mid- and late-Holocene sedimentary process and palaeovegetation changes near the mouth of the Amazon River. The Holocene 22, 359–370.

Guimarães, J.T.F., Souza-Filho, P.W.M., Alves, R., de Souza, E.B., da Costa, F.R., Reis, L.S., Sahoo, P.K., de Oliveira Manes, C.-L., Silva Júnior, R.O., Oti, D., Dall'Agnol, R., 2014. Source and distribution of pollen and spores in surface sediments of a plateau lake in southeastern Amazonia. Quaternary International 352, 181–196.

Haug, G.H., Hughen, K.A., Sigman, D.M., Peterson, L.C., Röhl, U., 2001. Southward migration of the intertropical convergence zone through the Holocene. Science 293, 1304–1308.

Hermanowski, B., da Costa, M.L., Behling, H., 2012a. Environmental changes in southeastern Amazonia during the last 25,000yr revealed from a paleoecological record. Quaternary Research 77, 138–148.

Hermanowski, B., da Costa, M.L., Behling, H., 2014. Possible linkages of palaeofires in southeast Amazonia to a changing climate since the Last Glacial Maximum. Vegetation History and Archaeobotany 1–14.

Hermanowski, B., da Costa, M.L., Carvalho, A.T., Behling, H., 2012b. Palaeoenvironmental dynamics and underlying climatic changes in southeast Amazonia (Serra Sul dos

1005 Carajás, Brazil) during the late Pleistocene and Holocene. Palaeogeography,
1006 Palaeoclimatology, Palaeoecology 365-366, 227–246.

1007 Hogg, A.G., Hua, Q., Blackwell, P.G., Niu, M., Buck, C.E., 2013. SHCal13 Southern
1008 Hemisphere calibration, 0–50,000 years cal BP. Radiocarbon 55, 1889–1903.

1009 Horák, I., Vidal-Torrado, P., Silva, A.C., Pessenda, L.C.R., 2011. Pedological and isotopic
1010 relations of a highland tropical peatland, Mountain Range of the Espinhaço Meridional
1011 (Brazil). Revista Brasileira de Ciência do Solo 35, 41–52.

1012 Horbe, A.M.C., Behling, H., Nogueira, A.C.R., Mapes, R., 2011. Environmental changes in
1013 the western Amazônia: morphological framework, geochemistry, palynology and
1014 radiocarbon dating data. 83, 863–874.

1015 Hueck, K., 1953. Distribuição e habitat natural do Pinheiro do Paraná (Araucaria
1016 angustifolia). Boletim da Faculdade de Filosofia, Ciências e Letras, Universidade de São
1017 Paulo. Botânica 10, 1–24.

1018 Huffman, G.J., Bolvin, D.T., Nelkin, E.J., Wolff, D.B., Adler, R.F., Gu, G., Hong, Y., Bowman,
1019 K.P., Stocker, E.F., 2007. The TRMM Multisatellite Precipitation Analysis (TMPA):
1020 Quasi-Global, Multiyear, Combined-Sensor Precipitation Estimates at Fine Scales.
1021 Journal of Hydrometeorology 8, 38–55.

1022 Huntingford, C., Zelazowski, P., Galbraith, D.R., Mercado, L.M., Sitch, S., Fisher, R.A.,
1023 Lomas, M., Walker, A.P., Jones, C.D., Booth, B.B.B., Malhi, Y., Hemming, D., Kay, G.,
1024 Good, P., Lewis, S.L., Phillips, O.L., Atkin, O.K., Lloyd, J., Gloor, E., Zaragoza-Castells,
1025 J., Meir, P., Betts, R.A., Harris, P.P., Nobre, C., Marengo, J.A., Cox, P.M., 2013.
1026 Simulated resilience of tropical rainforests to CO2-induced climate change. Nature
1027 Geoscience 6, 268–273.

1028 Iriarte, J., Behling, H., 2007. The expansion of Araucaria forest in the southern Brazilian

highlands during the last 4000 years and its implications for the development of the Taquara/Itararé …. Environmental archaeology 12, 115–127.

Iriarte, J., DeBlasis, P., Souza, J.G., Corteletti, R., 2016. Emergent Complexity, Changing Landscapes, and Spheres of Interaction in Southeastern South America During the Middle and Late Holocene. Journal of Archaeological Research 10.1007/s10814-016-9100-0, 1–63.

Irion, G., Bush, M.B., Nunes de Mello, J.A., Stüben, D., Neumann, T., Müller, G., Morais de, J.O., Junk, J.W., 2006. A multiproxy palaeoecological record of Holocene lake sediments from the Rio Tapajós, eastern Amazonia. Palaeogeography, Palaeoclimatology, Palaeoecology 240, 523–535.

Jeske-Pieruschka, V., Behling, H., 2011. Palaeoenvironmental history of the São Francisco de Paula region in southern Brazil during the late Quaternary inferred from the Rincão das Cabritas core. The Holocene 22, 0959683611414930–1262.

Jeske-Pieruschka, V., Fidelis, A., Bergamin, R.S., Vélez, E., Behling, H., 2010. Araucaria forest dynamics in relation to fire frequency in southern Brazil based on fossil and modern pollen data. Review of Palaeobotany and Palynology 160, 53–65.

Jeske-Pieruschka, V., Pillar, V.D., De Oliveira, M.A.T., Behling, H., 2012. New insights into vegetation, climate and fire history of southern Brazil revealed by a 40,000 year environmental record from the State Park Serra do Tabuleiro. Vegetation History and Archaeobotany 22, 299–314.

Joetzjer, E., Douville, H., Delire, C., Ciais, P., 2013. Present-day and future Amazonian precipitation in global climate models: CMIP5 versus CMIP3. Climate Dynamics 41, 2921–2936.

Joussaume, S., Taylor, K.E., 1995. Status of the Paleoclimate Modeling Intercomparison

1053 Project (PMIP). In: Monterey, CA.

1054 Kanner, L.C., Burns, S.J., Cheng, H., Edwards, R.L., Vuille, M., 2013. High-resolution
1055 variability of the South American summer monsoon over the last seven millennia:
1056 insights from a speleothem record from the central Peruvian Andes. Quaternary Science
1057 Reviews 75, 1–10.

1058 Killeen, T.J., Douglas, M., Consiglio, T., Jørgensen, P.M., Mejia, J., 2007. Dry spots and wet
1059 spots in the Andean hotspot. Journal of Biogeography 34, 1357–1373.

1060 Kipnis, R., Caldarelli, S.B., de Oliveira, W.C., 2005. Contribuição para a cronologia da
1061 colonização amazônica e suas implicações teóricas. Revista de Arqueologia 18, 81–93.

1062 Koutavas, A., Joanides, S., 2012. El Niño-Southern Oscillation extrema in the Holocene and
1063 Last Glacial Maximum. Paleoceanography 27, 1–15.

1064 Lachniet, M.S., 2009. Climatic and environmental controls on speleothem oxygen-isotope
1065 values. Quaternary Science Reviews 28, 412–432.

1066 Laurance, W.F., Delamônica, P., Laurance, S.G.W., Vasconcelos, H.L., Lovejoy, T.E., 2000.
1067 Rainforest fragmentation kills big trees. Nature 404, 836–836.

1068 Leal, M.G., Lorscheitter, M.L., 2007. Plant succession in a forest on the Lower Northeast
1069 Slope of Serra Geral, Rio Grande do Sul, and Holocene palaeoenvironments, Southern
1070 Brazil. Acta Botanica Brasilica 21, 1–10.

1071 Ledru, M.-P., 1993. Late Quaternary Environmental and Climatic Changes in Central Brazil.
1072 Quaternary Research 39, 90–98.

1073 Ledru, M.-P., Ceccantini, G., Gouveia, S.E.M., López-Sáez, J.A., Pessenda, L.C.R., Ribeiro,
1074 A.S., 2006. Millenial-scale climatic and vegetation changes in a northern Cerrado
1075 (Northeast, Brazil) since the Last Glacial Maximum. Quaternary Science Reviews 25,

1110–1126.

Ledru, M.-P., Mourguiart, P., Riccomini, C., 2009. Related changes in biodiversity, insolation and climate in the Atlantic rainforest since the last interglacial. Palaeogeography, Palaeoclimatology, Palaeoecology 271, 140–152.

Ledru, M.-P., Rousseau, D.D., Cruz, F.W., Riccomini, C., Karmann, I., Martin, L., 2005. Paleoclimate changes during the last 100,000 yr from a record in the Brazilian Atlantic rainforest region and interhemispheric comparison. Quaternary Research 64, 444–450.

Leonhardt, A., Lorscheitter, M.L., 2010. The last 25,000 years in the Eastern Plateau of Southern Brazil according to Alpes de São Francisco record. Journal of South American Earth Sciences 29, 454–463.

Levine, N.M., Zhang, K., Longo, M., Baccini, A., Phillips, O.L., Lewis, S.L., Alvarez-Dávila, E., Segalin de Andrade, A.C., Brienen, R.J.W., Erwin, T.L., Feldpausch, T.R., Monteagudo Mendoza, A.L., Núñez Vargas, P., Prieto, A., Silva-Espejo, J.E., Malhi, Y., Moorcroft, P.R., 2016. Ecosystem heterogeneity determines the ecological resilience of the Amazon to climate change. Proceedings of the National Academy of Sciences 113, 793–797.

Liu, K.-B., Colinvaux, P.A., 1988. A 5200-Year History of Amazon Rain Forest. Journal of Biogeography 15, 231.

Lorente, F.L., Pessenda, L.C.R., Oboh-Ikuenobe, F., Buso, A.A., Jr, Cohen, M.C.L., Meyer, K.E.B., Giannini, P.C.F., De Oliveira, P.E., Rossetti, D. de F., Borotti Filho, M.A., França, M.C., de Castro, D.F., Bendassolli, J.A., Macario, K., 2014. Palynofacies and stable C and N isotopes of Holocene sediments from Lake Macuco (Linhares, Espírito Santo, southeastern Brazil): Depositional settings and palaeoenvironmental evolution. Palaeogeography, Palaeoclimatology, Palaeoecology 415, 69–82.

Macedo, R.B., Souza, P.A., Bauermann, S.G., Bordignon, S.A.L., 2010. Palynological analysis of a late Holocene core from Santo Antônio da Patrulha, Rio Grande do Sul, Southern Brazil. 82, 731–745.

Maezumi, S.Y., Power, M.J., Mayle, F.E., McLauchlan, K.K., Iriarte, J., 2015. Effects of past climate variability on fire and vegetation in the cerrãdo savanna of the Huanchaca Mesetta, NE Bolivia. Climate of the Past 11, 835–853.

Malhi, Y., Phillips, O.L., Lloyd, J., Baker, T., Wright, J., Almeida, S., Arroyo, L., Frederiksen, T., Grace, J., Higuchi, N., Killeen, T.J., Laurance, W.F., Leaño, C., Lewis, S.L., Meir, P., Monteagudo, A., Neill, D., Vargas, P.N., Panfil, S.N., Patino, S., Pitman, N., Quesada, C.A., Rudas-Ll, A., Salomão, R., Saleska, S., Silva, N., Silveira, M., Sombroek, W.G., Valencia, R., Martínez, R.V., Vieira, I.C.G., Vinceti, B., 2002. An international network to monitor the structure, composition and dynamics of Amazonian forests (RAINFOR). Journal of Vegetation Science 13, 439–450.

Malhi, Y., Roberts, J.T., Betts, R.A., Killeen, T.J., Li, W., Nobre, C.A., 2008. Climate change, deforestation, and the fate of the Amazon. Science 319, 169–172.

Marchant, R., Cleef, A., Harrison, S.P., Hooghiemstra, H., Markgraf, V., van Boxel, J., Ager, T., Almeida, L., Anderson, R., Baied, C., Behling, H., Berrio, J.C., Burbridge, R.E., Björck, S., Byrne, R., Bush, M.B., Duivenvoorden, J., Flenley, J., De Oliveira, P.E., van Geel, B., Graf, K., Gosling, W.D., Harbele, S., van der Hammen, T., Hansen, B., Horn, S., Kuhry, P., Ledru, M.-P., Mayle, F.E., Leyden, B., Lozano-Garcia, S., Melief, A.M., Moreno, P., Moar, N.T., Prieto, A., van Reenen, G., Salgado-Labouriau, M.L., Schäbitz, F., Schreve-Brinkman, E.J., Wille, M., 2009. Pollen-based biome reconstructions for Latin America at 0, 6000 and 18 000 radiocarbon years ago. 5, 369–461.

Marengo, J.A., Douglas, M.W., Dias, P.L.S., 2002. The South American low-level jet east of the Andes during the 1999 LBA-TRMM and LBA-WET AMC campaign. Journal of

Geophysical Research 107, 8079.

Mayle, F.E., Burbridge, R.E., Killeen, T.J., 2000. Millennial-scale dynamics of southern Amazonian rain forests. Science 290, 2291–2294.

Mayle, F.E., Power, M.J., 2008. Impact of a drier Early-Mid-Holocene climate upon Amazonian forests. Philosophical Transactions of the Royal Society B: Biological Sciences 363, 1829–1838.

McMichael, C.N.H., Bush, M.B., Piperno, D.R., Silman, M.R., Zimmerman, A.R., Anderson, C., 2012. Spatial and temporal scales of pre-Columbian disturbance associated with western Amazonian lakes. The Holocene 22, 131–141.

Metcalfe, S.E., Whitney, B.S., Fitzpatrick, K.A., Mayle, F.E., Loader, N.J., Street-Perrott, F.A., Mann, D.G., 2014. Hydrology and climatology at Laguna La Gaiba, lowland Bolivia: complex responses to climatic forcings over the last 25 000 years. Journal of Quaternary Science 29, 289–300.

Meyers, P.A., 1994. Preservation of elemental and isotopic source identification of sedimentary organic matter. Chemical Geology 114, 289–302.

Montade, V., Ledru, M.-P., Burte, J., Martins, E.S.P.R., Verola, C.F., da Costa, I.R., Silva, F.H.M.E., 2014. Stability of a Neotropical microrefugium during climatic instability. Journal of Biogeography 41, 1215–1226.

Morrás, H., Moretti, L., Píccolo, G., Zech, W., 2009. Genesis of subtropical soils with stony horizons in NE Argentina: Autochthony and polygenesis. Quaternary International 196, 137–159.

Moy, C.M., Seltzer, G.O., Rodbell, D.T., Anderson, D.M., 2002. Variability of El Nino/Southern Oscillation activity at millennial timescales during the Holocene epoch. Nature 420, 162–165.

1149 Nuno Veríssimo, P., Safford, H.D., Behling, H., 2012. Holocene vegetation and fire history of
1150 the Serra do Caparao, SE Brazil. The Holocene 22, 1243–1250.

1151 Olson, D.M., Dinerstein, E., Wikramanayake, E.D., Burgess, N.D., Powell, G.V.N.,
1152 Underwood, E.C., D'amico, J.A., Itoua, I., Strand, H.E., Morrison, J.C., Loucks, C.J.,
1153 Allnutt, T.F., Ricketts, T.H., Kura, Y., Lamoreux, J.F., Wettengel, W.W., Hedao, P.,
1154 Kassem, K.R., 2001. Terrestrial Ecoregions of the World: A New Map of Life on Earth A
1155 new global map of terrestrial ecoregions provides an innovative tool for conserving
1156 biodiversity. BioScience 51, 933–938.

1157 Parizzi, M.G., Salgado-Labouriau, M.L., Kohler, H.C., 1998. Genesis and environmental
1158 history of Lagoa Santa, southeastern Brazil. The Holocene 8, 311–321.

1159 Pennington, R.T., Prado, D.E., Pendry, C.A., 2000. Neotropical seasonally dry forests and
1160 Quaternary vegetation changes. Journal of Biogeography 27, 261–273.

1161 Pessenda, L.C.R., 2004. Holocene fire and vegetation changes in southeastern Brazil as
1162 deduced from fossil charcoal and soil carbon isotopes. Quaternary International 114,
1163 35–43.

1164 Pessenda, L.C.R., Boulet, R., Aravena, R., Rosolen, V., Gouveia, S.E.M., Ribeiro, A.S.,
1165 Lamotte, M., 2001. Origin and dynamics of soil organic matter and vegetation changes
1166 during the Holocene in a forest-savanna transition zone, Brazilian Amazon region. The
1167 Holocene 11, 250–254.

1168 Pessenda, L.C.R., De Oliveira, P.E., Mofatto, M., de Medeiros, V.B., Francischetti Garcia,
1169 R.J., Aravena, R., Bendassolli, J.A., Zuniga Leite, A., Saad, A.R., Lincoln Etchebehere,
1170 M., 2009. The evolution of a tropical rainforest/grassland mosaic in southeastern Brazil
1171 since 28,000 14C yr BP based on carbon isotopes and pollen records. Quaternary
1172 Research 71, 437–452.

1173 Pessenda, L.C.R., Gomes, B.M., Aravena, R., Ribeiro, A.S., Boulet, R., Gouveia, S.E.M.,
1174 1998. The carbon isotope record in soils along a forest-cerrado ecosystem transect:
1175 implications for vegetation changes in the Rondonia state, southwestern Brazilian
1176 Amazon region. The Holocene 8, 599–603.

1177 Pessenda, L.C.R., Gouveia, S.E.M., Ribeiro, A. de S., De Oliveira, P.E., Aravena, R., 2010.
1178 Late Pleistocene and Holocene vegetation changes in northeastern Brazil determined
1179 from carbon isotopes and charcoal records in soils. Palaeogeography,
1180 Palaeoclimatology, Palaeoecology 297, 597–608.

1181 Pessenda, L.C.R., Ledru, M.-P., Gouveia, S.E.M., Aravena, R., Ribeiro, A.S., Bendassolli,
1182 J.A., Boulet, R., 2005. Holocene palaeoenvironmental reconstruction in northeastern
1183 Brazil inferred from pollen, charcoal and carbon isotope records. The Holocene 15, 812–
1184 820.

1185 Pessenda, L.C.R., Ribeiro, A. de S., Gouveia, S.E.M., Aravena, R., Boulet, R., Bendassolli,
1186 J.A., 2004. Vegetation dynamics during the late Pleistocene in the Barreirinhas region,
1187 Maranhão State, northeastern Brazil, based on carbon isotopes in soil organic matter.
1188 Quaternary Research 62, 183–193.

1189 Phillips, O.L., Aragão, L.E.O.C., Lewis, S.L., Fisher, J.B., Lloyd, J., Lopez-Gonzalez, G.,
1190 Malhi, Y., Monteagudo, A., Peacock, J., Quesada, C.A., van der Heijden, G., Almeida,
1191 S., Amaral, I., Arroyo, L., Aymard, G., Baker, T.R., Banki, O., Blanc, L., Bonal, D.,
1192 Brando, P.M., Chave, J., de Oliveira, A.C.A., Cardozo, N.D., Czimczik, C.I., Feldpausch,
1193 T.R., Freitas, M.A., Gloor, E., Higuchi, N., Jimenez, E., Lloyd, G., Meir, P., Mendoza, C.,
1194 Morel, A., Neill, D.A., Nepstad, D., Patino, S., Penuela, M.C., Prieto, A., Ramírez, F.,
1195 Schwarz, M., Silva, J., Silveira, M., Thomas, A.S., Steege, ter, H., Stropp, J., Vasquez,
1196 R., Zelazowski, P., Davila, E.A., Andelman, S., Andrade, A.S., Chao, K.J., Erwin, T., Di
1197 Fiore, A., Coronado, E.N.H., Keeling, H., Killeen, T.J., Laurance, W.F., Cruz, A.P.,
1198 Pitman, N.C.A., Vargas, P.N., Ramirez-Angulo, H., Rudas, A., Salamao, R., Silva, N.,

Terborgh, J., Torres-Lezama, A., 2009. Drought Sensitivity of the Amazon Rainforest. Science 323, 1344–1347.

Piperno, D.R., 2006. Phytoliths: A Comprehensive Guide for Archaeologists and Paleoecologists. Altamira Press, Lanham, MD.

Pires, G.L.P., Meyer, K.E.B., Gomes, M.O.S., 2016. Palinologia da Vereda Juquinha/Cuba, Parque Estadual da Serra do Cabral, Minas Gerais, Brasil. Revista Brasileira de Paleontologia 19, 95–110.

Power, M.J., Marlon, J., Ortiz, N., Bartlein, P.J., Harrison, S.P., Mayle, F.E., Ballouche, A., Bradshaw, R.H.W., Carcaillet, C., Cordova, C., Mooney, S., Moreno, P.I., Prentice, I.C., Thonicke, K., Tinner, W., Whitlock, C., Zhang, Y., Zhao, Y., Ali, A.A., Anderson, R.S., Beer, R., Behling, H., Briles, C., Brown, K.J., Brunelle, A., Bush, M.B., Camill, P., Chu, G.Q., Clark, J., Colombaroli, D., Connor, S., Daniau, A.L., Daniels, M., Dodson, J., Doughty, E., Edwards, M.E., Finsinger, W., Foster, D., Frechette, J., Gaillard, M.J., Gavin, D.G., Gobet, E., Haberle, S., Hallett, D.J., Higuera, P., Hope, G., Horn, S., Inoue, J., Kaltenrieder, P., Kennedy, L., Kong, Z.C., Larsen, C., Long, C.J., Lynch, J., Lynch, E.A., McGlone, M., Meeks, S., Mensing, S., Meyer, G., Minckley, T., Mohr, J., Nelson, D.M., New, J., Newnham, R., Noti, R., Oswald, W., Pierce, J., Richard, P.J.H., Rowe, C., Goñi, M.F.S., Shuman, B.N., Takahara, H., Toney, J., Turney, C., Urrego-Sanchez, D.H., Umbanhowar, C., Vandergoes, M., Vanniere, B., Vescovi, E., Walsh, M., Wang, X., Williams, N., Wilmshurst, J., Zhang, J.H., 2008. Changes in fire regimes since the Last Glacial Maximum: an assessment based on a global synthesis and analysis of charcoal data. Climate Dynamics 30, 887–907.

Prado, D.E., Gibbs, P.E., 1993. Patterns of Species Distributions in the Dry Seasonal Forests of South America. Annals of the Missouri Botanical Garden 80, 902–28.

Prado, L.F., Wainer, I., Chiessi, C.M., 2013a. Mid-Holocene PMIP3/CMIP5 model results:

1224 Intercomparison for the South American Monsoon System. The Holocene 23, 1915–
1225 1920.

1226 Prado, L.F., Wainer, I., Chiessi, C.M., Ledru, M.-P., Turcq, B., 2013b. A mid-Holocene
1227 climate reconstruction for eastern South America. 9, 2117–2133.

1228 Prentice, I.C., 1985. Pollen representation, source area, and basin size: toward a unified
1229 theory of pollen analysis. Quaternary Research 23, 76–86.

1230 Prentice, I.C., Guiot, J., Huntley, B., Jolly, D., Cheddadi, R., 1996. Reconstructing biomes
1231 from palaeoecological data: a general method and its application to European pollen
1232 data at 0 and 6 ka. Climate Dynamics 12, 185–194.

1233 Prentice, I.C., Webb, T., III, 1998. BIOME 6000: reconstructing global mid- Holocene
1234 vegetation patterns from palaeoecological records. Journal of Biogeography 25, 997–
1235 1005.

1236 Raczka, M.F., De Oliveira, P.E., Bush, M.B., McMichael, C.N.H., 2013. Two paleoecological
1237 histories spanning the period of human settlement in southeastern Brazil. Journal of
1238 Quaternary Science 28, 144–151.

1239 Raia, A., Cavalcanti, I.F.A., 2008. The Life Cycle of the South American Monsoon System.
1240 Journal of Climate 21, 6227–6246.

1241 Rammig, A., Jupp, T., Thonicke, K., Tietjen, B., Heinke, J., Ostberg, S., Lucht, W., Cramer,
1242 W., Cox, P.M., 2010. Estimating the risk of Amazonian forest dieback. The New
1243 phytologist 187, 694–706.

1244 Reimer, P.J., Bard, E., Bayliss, A., Beck, J.W., Blackwell, P.G., Ramsey, C.B., Buck, C.E.,
1245 Cheng, H., Edwards, R.L., Friedrich, M., Grootes, P.M., Guilderson, T.P., Haflidason, H.,
1246 Hajdas, I., Hatté, C., Heaton, T.J., Hoffmann, D.L., Hogg, A.G., Hughen, K.A., Kaiser,
1247 K.F., Kromer, B., Manning, S.W., Niu, M., Reimer, R.W., Richards, D.A., Scott, E.M.,

1248 Southon, J.R., Staff, R.A., Turney, C.S.M., van der Plicht, J., 2013. IntCal13 and
1249 Marine13 Radiocarbon Age Calibration Curves 0–50,000 Years cal BP. Radiocarbon 55,
1250 1869–1887.

1251 Rodrigues-Filho, S., Behling, H., Irion, G., Müller, G., 2002. Evidence for Lake Formation as
1252 a Response to an Inferred Holocene Climatic Transition in Brazil. Quaternary Research
1253 57, 131–137.

1254 Rowe, H.D., Dunbar, R.B., Mucciarone, D.A., Seltzer, G.O., Baker, P.A., Fritz, S., 2002.
1255 Insolation, moisture balance and climate change on the South American Altiplano since
1256 the last glacial maximum. Climatic change 52, 175–199.

1257 Rowland, L., da Costa, A.C.L., Galbraith, D.R., Oliveira, R.S., Binks, O.J., Oliveira, A.A.R.,
1258 Pullen, A.M., Doughty, C.E., Metcalfe, D.B., Vasconcelos, S.S., Ferreira, L.V., Malhi, Y.,
1259 Grace, J., Mencuccini, M., Meir, P., 2015. Death from drought in tropical forests is
1260 triggered by hydraulics not carbon starvation. Nature 1–13.

1261 Saha, S., Moorthi, S., Pan, H.-L., Wu, X., Wang, J., Nadiga, S., Tripp, P., Kistler, R.,
1262 Woollen, J., Behringer, D., Liu, H., Stokes, D., Grumbine, R., Gayno, G., Wang, J., Hou,
1263 Y.-T., Chuang, H.-Y., Juang, H.-M.H., Sela, J., Iredell, M., Treadon, R., Kleist, D., Delst,
1264 P.V., Keyser, D., Derber, J., Ek, M., Meng, J., Wei, H., Yang, R., Lord, S., van den Dool,
1265 H., Kumar, A., Wang, W., Long, C., Chelliah, M., Xue, Y., Huang, B., Schemm, J.-K.,
1266 Ebisuzaki, W., Lin, R., Xie, P., Chen, M., Zhou, S., Higgins, W., Zou, C.-Z., Liu, Q.,
1267 Chen, Y., Han, Y., Cucurull, L., Reynolds, R.W., Rutledge, G., Goldberg, M., 2010a.
1268 NCEP Climate Forecast System Reanalysis (CFSR) Monthly Products, January 1979 to
1269 December 2010. Research Data Archive at the National Center for Atmospheric
1270 Research, Computational and Information Systems Laboratory, Boulder, CO.

1271 Saha, S., Moorthi, S., Pan, H.-L., Wu, X., Wang, J., Nadiga, S., Tripp, P., Kistler, R.,
1272 Woollen, J., Behringer, D., Liu, H., Stokes, D., Grumbine, R., Gayno, G., Wang, J., Hou,

Y.-T., Chuang, H.-Y., Juang, H.-M.H., Sela, J., Iredell, M., Treadon, R., Kleist, D., Van Delst, P., Keyser, D., Derber, J., Ek, M., Meng, J., Wei, H., Yang, R., Lord, S., van den Dool, H., Kumar, A., Wang, W., Long, C., Chelliah, M., Xue, Y., Huang, B., Schemm, J.-K., Ebisuzaki, W., Lin, R., Xie, P., Chen, M., Zhou, S., Higgins, W., Zou, C.-Z., Liu, Q., Chen, Y., Han, Y., Cucurull, L., Reynolds, R.W., Rutledge, G., Goldberg, M., 2010b. The NCEP Climate Forecast System Reanalysis. Bull. Amer. Meteor. Soc. 91, 1015–1057.

Saia, S.E.M.G., Pessenda, L.C.R., Gouveia, S.E.M., Aravena, R., Bendassolli, J.A., 2008. Last glacial maximum (LGM) vegetation changes in the Atlantic Forest, southeastern Brazil. Quaternary International 184, 195–201.

Sampaio, E.V.S.B., 1995. Overview of the Brazilian caatinga. In: Bullock, S.H., Mooney, H.A., Medina, E. (Eds.), Seasonally Dry Tropical Forests. Cambridge University Press, Cambridge, United Kingdom, pp. 35–63.

Seltzer, G.O., Rodbell, D., Burns, S., 2000. Isotopic evidence for late Quaternary climatic change in tropical South America. Geology 28, 35–38.

Sifeddine, A., Albuquerque, A.L.S., Ledru, M.-P., 2003. A 21 000 cal years paleoclimatic record from Caçó Lake, northern Brazil: evidence from sedimentary and pollen analyses. Palaeogeography, Palaeoclimatology, Palaeoecology 189, 25–34.

Sifeddine, A., Bertrand, P., Fournier, M., 1994. La sédimentation organique lacustre en milieu tropical humide (Carajás, Amazonie orientale, Brésil): relation avec les changements climatiques au cours des 60 000 dernières années. Bulletin de la Societe geologique de France 165, 613–621.

Sifeddine, A., Martin, L., Turcq, B., Volkmer-Ribeiro, C., Soubiès, F., Cordeiro, R.C., Suguio, K., 2001. Variations of the Amazonian rainforest environment: a sedimentological record covering 30,000 years. Palaeogeography, Palaeoclimatology, Palaeoecology 168, 221–235.

1298 Sifeddine, A., Wirrmann, D., Albuquerque, A.L.S., Turcq, B., Cordeiro, R.C., Gurgel, M.H.C.,
1299 Abrão, J.J., 2004. Bulk composition of sedimentary organic matter used in
1300 palaeoenvironmental reconstructions: examples from the tropical belt of South America
1301 and Africa. Palaeogeography, Palaeoclimatology, Palaeoecology 214, 41–53.

1302 Silva, J.M.C.D., Bates, J.M., 2002. Biogeographic Patterns and Conservation in the South
1303 American Cerrado: A Tropical Savanna Hotspot. BioScience 52, 225–233.

1304 Silva, L., Sternberg, L., Haridasan, M., 2008. Expansion of gallery forests into central
1305 Brazilian savannas. Global Change Biology 14, 2108–2118.

1306 Silva, V.B.S., Kousky, V.E., 2012. The South American Monsoon System: Climatology and
1307 Variability. In: Wang, S., Gillies, R.R. (Eds.), Modern Climatology. pp. 123–152.

1308 Spracklen, D.V., Arnold, S.R., Taylor, C.M., 2012. Observations of increased tropical rainfall
1309 preceded by air passage over forests. Nature 489, 282–285.

1310 Sugita, S., 1993. A model of pollen source area for an entire lake surface. Quaternary
1311 Research 39, 239–244.

1312 Sugita, S., 1994. Pollen Representation of Vegetation in Quaternary Sediments - Theory and
1313 Method in Patchy Vegetation. Journal of Ecology 82, 881–897.

1314 Sugita, S., 2007a. Theory of quantitative reconstruction of vegetation I: pollen from large
1315 sites REVEALS regional vegetation composition. The Holocene 17, 229–241.

1316 Sugita, S., 2007b. Theory of quantitative reconstruction of vegetation II: all you need is
1317 LOVE. The Holocene 17, 243–257.

1318 Taylor, Z.P., Horn, S.P., Mora, C.I., Orvis, K.H., Cooper, L.W., 2010. A multi-proxy
1319 palaeoecological record of late-Holocene forest expansion in lowland Bolivia.
1320 Palaeogeography, Palaeoclimatology, Palaeoecology 293, 98–107.

1321 Turcq, B., Albuquerque, A.L.S., Cordeiro, R.C., Sifeddine, A., Simoes Filho, F.F.L., Souza,
1322 A.G., Abrão, J.J., Oliveira, F.B.L., Silva, A.O., Capitâneo, J., 2002. Accumulation of
1323 organic carbon in five Brazilian lakes during the Holocene. Sedimentary Geology 148,
1324 319–342.

1325 Urrego, D.H., Bush, M.B., Silman, M.R., Niccum, B.A., La Rosa, P., McMichael, C.N.H.,
1326 Hagen, S., Palace, M., 2013. Holocene fires, forest stability and human occupation in
1327 south- western Amazonia. Journal of Biogeography 40, 521–533.

1328 van Breukelen, M.R., Vonhof, H.B., Hellstrom, J.C., Wester, W.C.G., Kroon, D., 2008. Fossil
1329 dripwater in stalagmites reveals Holocene temperature and rainfall variation in
1330 Amazonia. Earth and Planetary Science Letters 275, 54–60.

1331 Vuille, M., Burns, S.J., Taylor, B.L., Cruz, F.W., Bird, B.W., Abbott, M.B., Kanner, L.C.,
1332 Cheng, H., Novello, V.F., 2012. A review of the South American monsoon history as
1333 recorded in stable isotopic proxies over the past two millennia. Climate of the Past 8,
1334 1309–1321.

1335 Wang, X., Auler, A.S., Edwards, R.L., Cheng, H., Ito, E., Wang, Y., Kong, X., Solheid, M.,
1336 2007. Millennial-scale precipitation changes in southern Brazil over the past 90,000
1337 years. Geophysical Research Letters 34, L23701.

1338 Wang, X., Edwards, R.L., Auler, A.S., Cheng, H., Kong, X., Wang, Y., Cruz, F.W., Dorale,
1339 J.A., Chiang, H.-W., 2017. Hydroclimate changes across the Amazon lowlands over the
1340 past 45,000 years. Nature 541, 204–207.

1341 Watling, J., Iriarte, J., Mayle, F.E., Schaan, D., Pessenda, L.C.R., Loader, N.J., Street-
1342 Perrott, F.A., Dickau, R.E., Damasceno, A., Ranzi, A., 2017. Impact of pre-Columbian
1343 “geoglyph” builders on Amazonian forests. Proceedings of the National Academy of
1344 Sciences 114, 1868–1873.

1345 Watling, J., Iriarte, J., Whitney, B.S., Consuelo, E., Mayle, F.E., Castro, W., Schaan, D.,
1346 Feldpausch, T.R., 2016. Differentiation of neotropical ecosystems by modern soil
1347 phytolith assemblages and its implications for palaeoenvironmental and archaeological
1348 reconstructions II: Southwestern Amazonian forests. Review of Palaeobotany and
1349 Palynology 226, 30–43.

1350 Weng, C., Bush, M.B., Athens, J.S., 2002. Holocene climate change and hydrarch
1351 succession in lowland Amazonian Ecuador. Review of Palaeobotany and Palynology
1352 120, 73–90.

1353 Werneck, F.P., 2011. The diversification of eastern South American open vegetation
1354 biomes: Historical biogeography and perspectives. Quaternary Science Reviews 30,
1355 1630–1648.

1356 Whitney, B.S., Mayle, F.E., 2012. Pediastrum species as potential indicators of lake-level
1357 change in tropical South America. Journal of Paleolimnology 47, 601–615.

1358 Whitney, B.S., Mayle, F.E., Punyasena, S.W., Fitzpatrick, K.A., Burn, M.J., Guillen, R.,
1359 Chavez, E., Mann, D., Pennington, R.T., Metcalfe, S.E., 2011. A 45kyr palaeoclimate
1360 record from the lowland interior of tropical South America. Palaeogeography,
1361 Palaeoclimatology, Palaeoecology 307, 177–192.

1362 Ybert, J.-P., Turcq, B., Albuquerque, A.L., Cocquit, C., 2000. Evolution paléoécologique et
1363 paléoclimatique holocène dans la région moyenne du Rio Doce (Minas Gerais, Brésil)
1364 déduite de l'analyse palynologique de deux carottes du lac Dom Helvécio. In:
1365 Dynamique à long terme des écosystèmes forestiers intertropicaux. pp. 413–421.

1366 Zech, M., Zech, R., Morrás, H., Moretti, L., Glaser, B., Zech, W., 2009. Late Quaternary
1367 environmental changes in Misiones, subtropical NE Argentina, deduced from multi-proxy
1368 geochemical analyses in a palaeosol-sediment sequence. Quaternary International 196,
1369 121–136.

1370 Zhou, J., Lau, K.M., 1998. Does a monsoon climate exist over South America? Journal of
1371 Climate 11, 1020–1040.

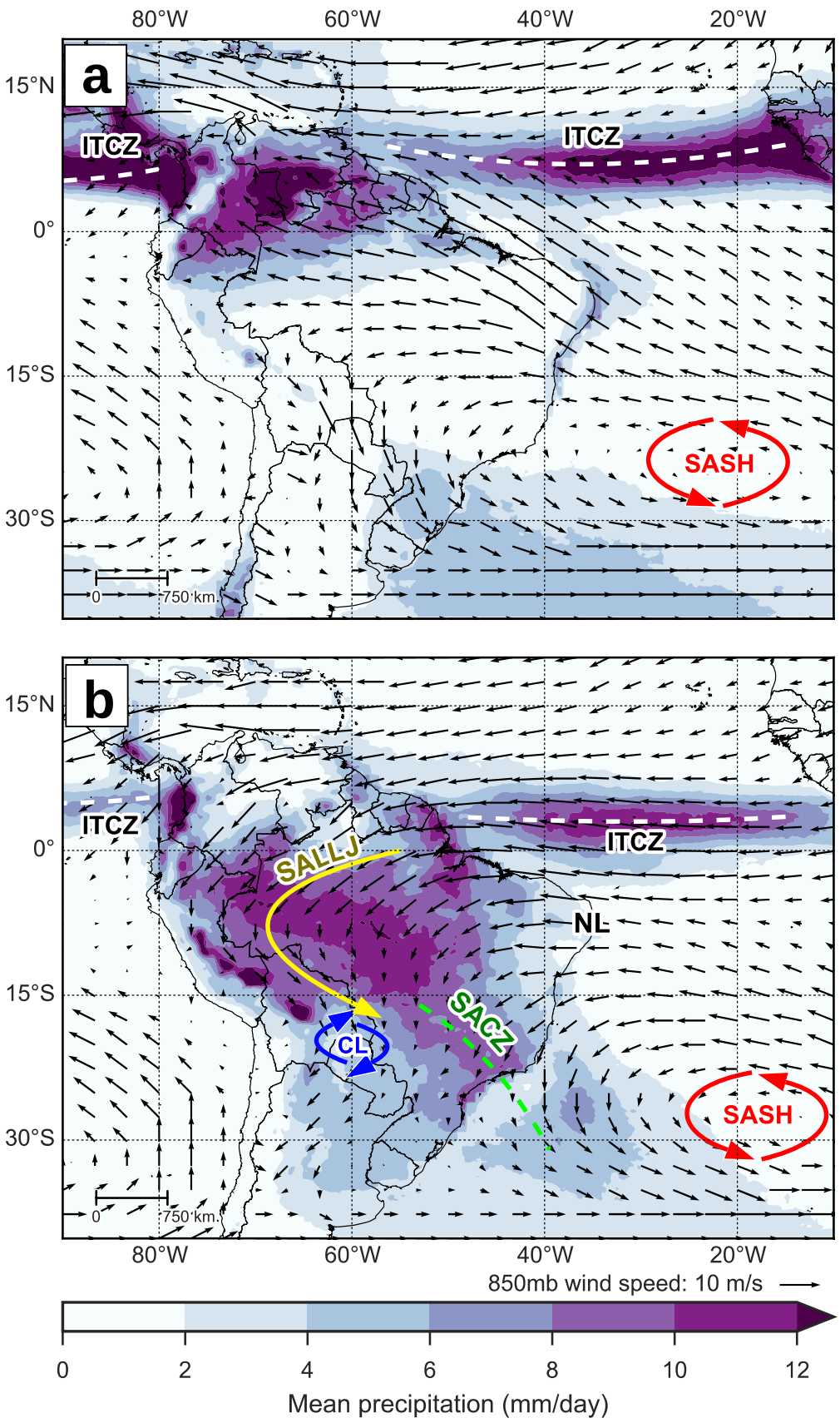
80°W
60°W
40°W
20°W
a
15°N
0°
15°S
30°S
ITCZ
ITCZ
SASH
0
750 km
b
ITCZ
ITCZ
SALLJ
NL
SACZ
CL
SASH
850mb wind speed: 10 m/s
0
2
4
6
8
10
12
Mean precipitation (mm/day)

Figure 1.

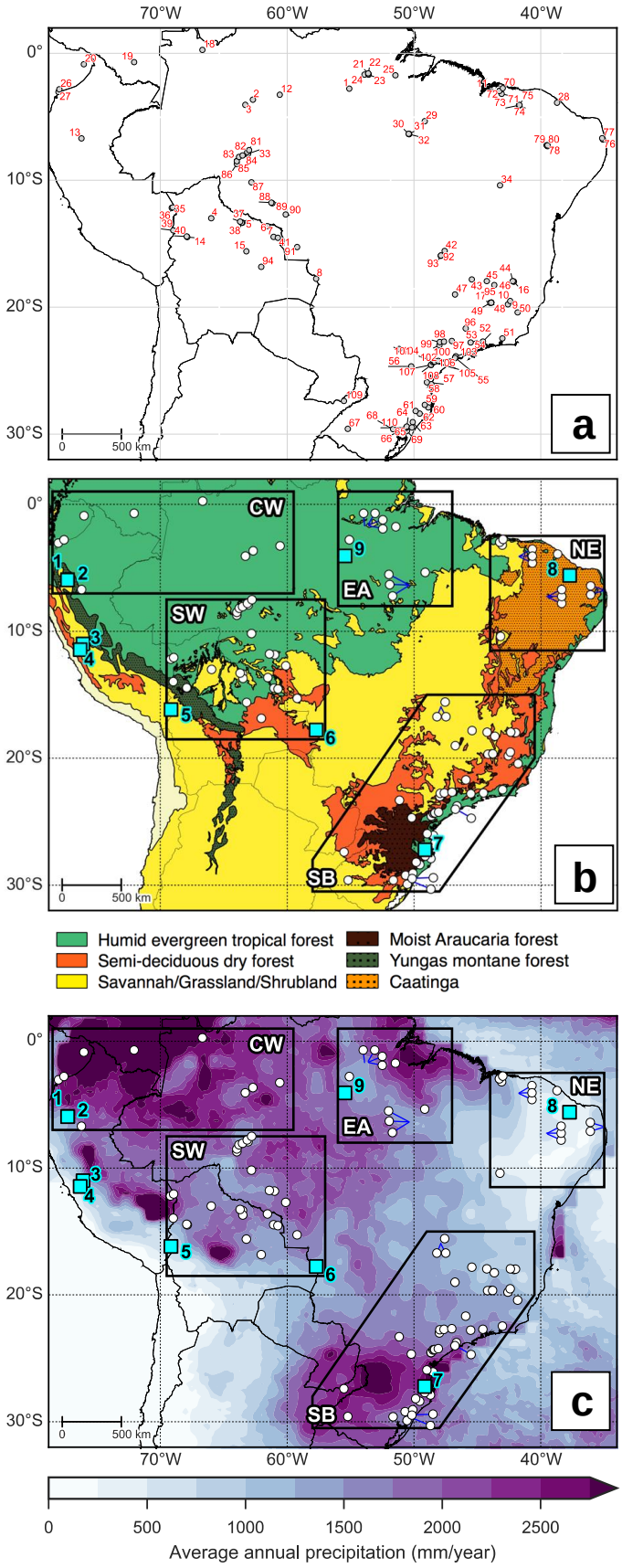
70°W
60°W
50°W
40°W
0°
10°S
20°S
30°S
0
500 km
a
CW
EA
NE
SW
SB
1
2
3
4
5
6
7
8
9
b
Humid evergreen tropical forest
Semi-deciduous dry forest
Savannah/Grassland/Shrubland
Moist Araucaria forest
Yungas montane forest
Caatinga
c
0
500
1000
1500
2000
2500
Average annual precipitation (mm/year)

Figure 2.

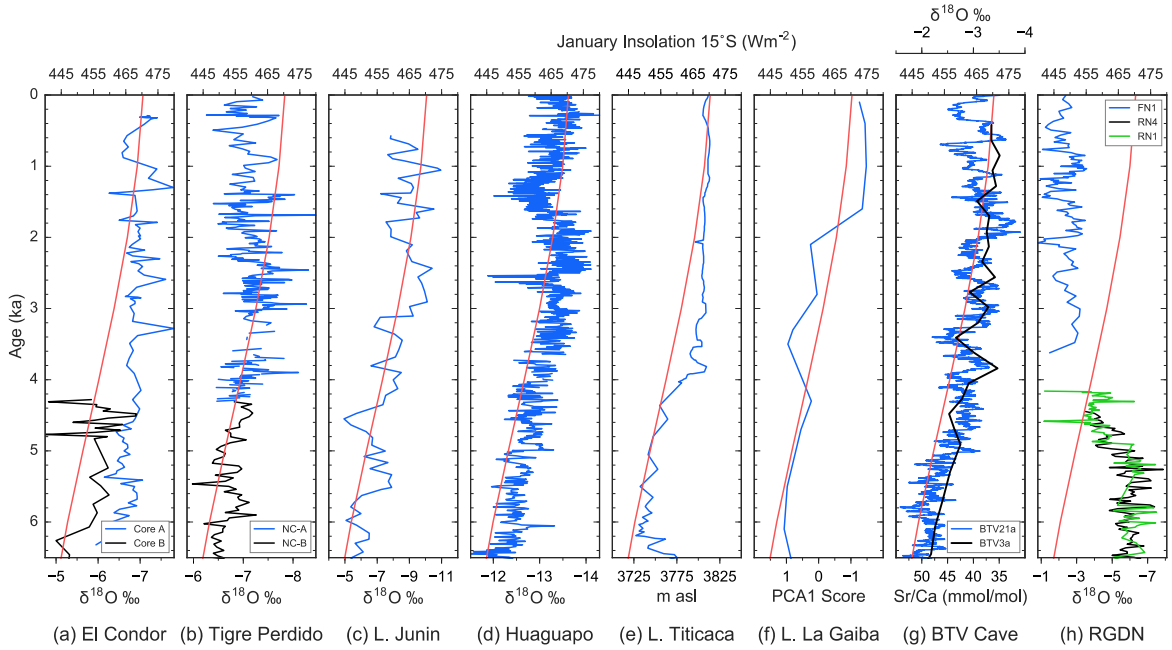
January Insolation 15°S (Wm-2)
δ18O ‰
Age (ka)
Core A
Core B
NC-A
NC-B
FN1
RN4
RN1
BTV21a
BTV3a
δ18O ‰
m asl
PCA1 Score
Sr/Ca (mmol/mol)
(a) El Condor
(b) Tigre Perdido
(c) L. Junin
(d) Huaguapo
(e) L. Titicaca
(f) L. La Gaiba
(g) BTV Cave
(h) RGDN

Figure 3.

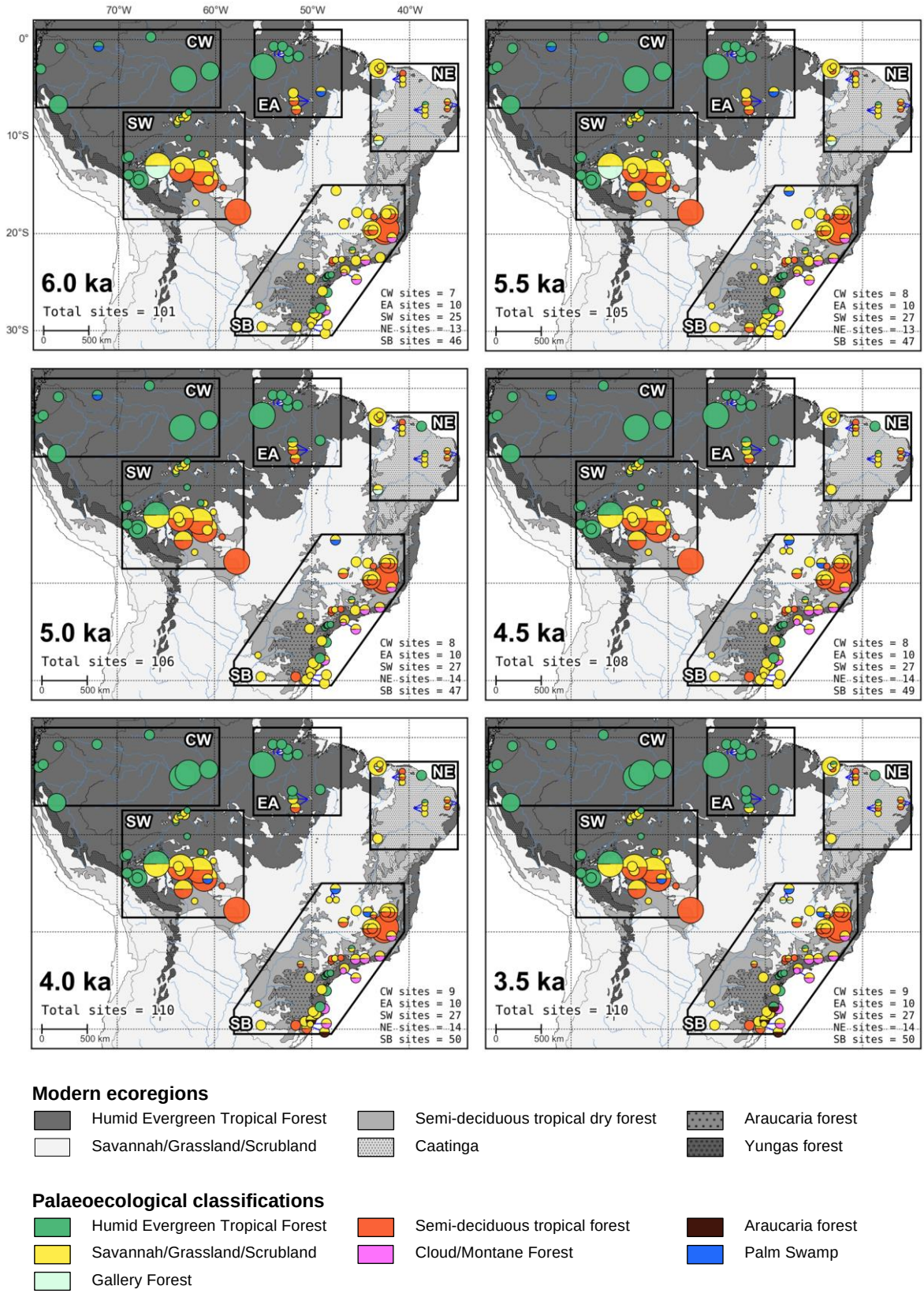
70°W
60°W
50°W
40°W
0°
10°S
20°S
30°S
CW
EA
NE
SW
SB
6.0 ka
Total sites = 101
CW sites = 7
EA sites = 10
SW sites = 25
NE sites = 13
SB sites = 46
5.5 ka
Total sites = 105
CW sites = 8
EA sites = 10
SW sites = 27
NE sites = 13
SB sites = 47
5.0 ka
Total sites = 106
CW sites = 8
EA sites = 10
SW sites = 27
NE sites = 14
SB sites = 47
4.5 ka
Total sites = 108
CW sites = 8
EA sites = 10
SW sites = 27
NE sites = 14
SB sites = 49
4.0 ka
Total sites = 110
CW sites = 9
EA sites = 10
SW sites = 27
NE sites = 14
SB sites = 50
3.5 ka
Total sites = 110
CW sites = 9
EA sites = 10
SW sites = 27
NE sites = 14
SB sites = 50
0
500 km
Modern ecoregions
Humid Evergreen Tropical Forest
Savannah/Grassland/Scrubland
Semi-deciduous tropical dry forest
Caatinga
Araucaria forest
Yungas forest
Palaeoecological classifications
Humid Evergreen Tropical Forest
Savannah/Grassland/Scrubland
Gallery Forest
Semi-deciduous tropical forest
Cloud/Montane Forest
Araucaria forest
Palm Swamp

Figure 4.

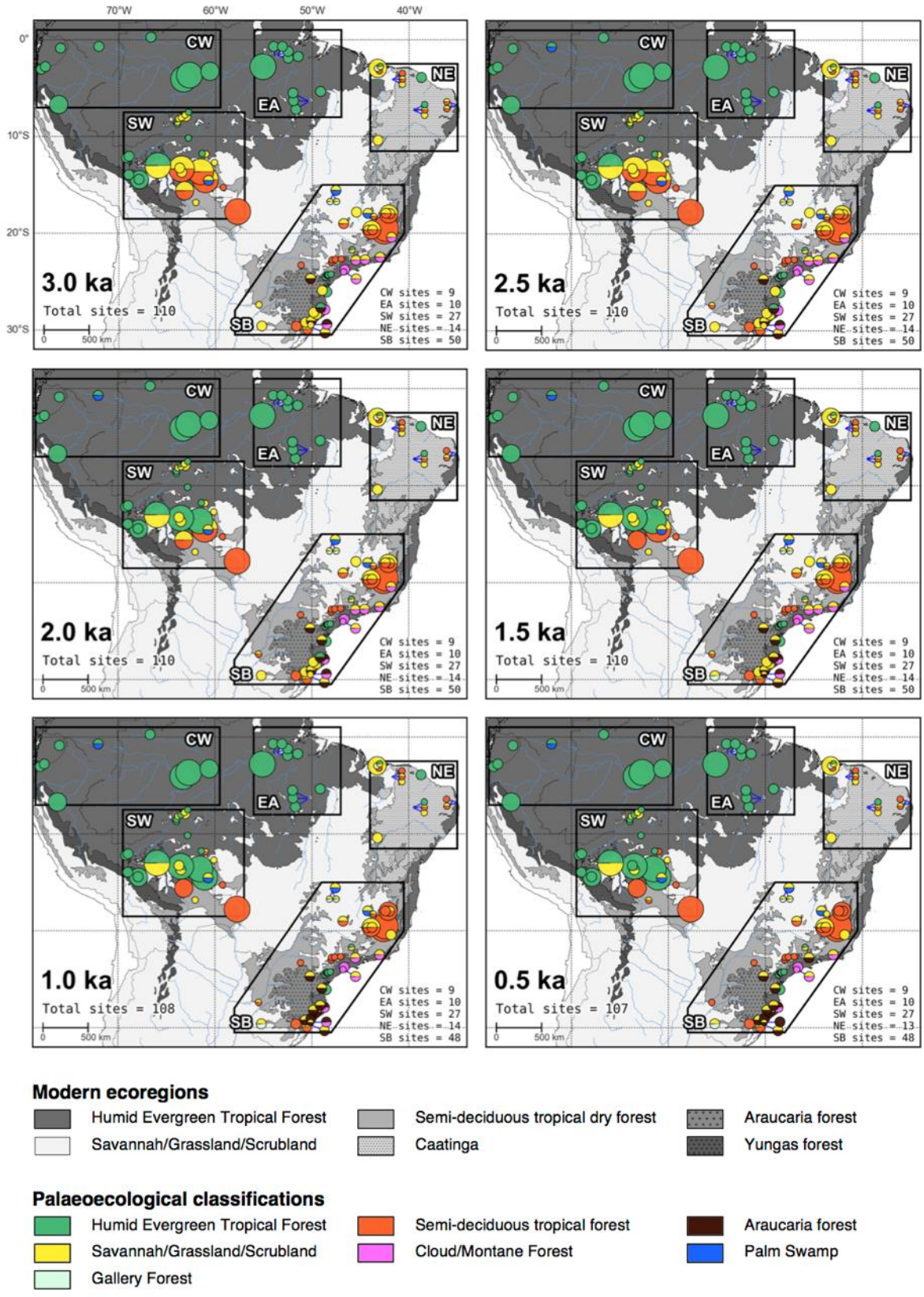

Figure 4. (continued)

Table 1.

ID	Site Name	Latitude	Longitude	Reference(s)
Size category: Large (L)				
1	Lago Tapajós TAP02 ***1,2,3,4***	2°47.14'S	55°6.13'W	(Irion et al., 2006)
2*	Acará lake ***1,3,4***	3°39.32'S	62°42.07'W	(Horbe et al., 2011)
3*	Coari Lake ***1,3,4***	4°3.85'S	63°18.11'W	(Horbe et al., 2011)
4	Lago Rogaguado ***1,2***	12°59.84'S	65°59.16'W	(Brugger et al., 2016)
5	Laguna Orícore ***1,2***	13°20.74'S	63°31.53'W	(Carson et al., 2014)
6	Laguna Bella Vista ***1,2***	13°37.00'S	61°33.00'W	(Mayle et al., 2000; Burbridge et al., 2004)
7	Laguna Chaplin ***1,2***	14°28.00'S	61°4.00'W	(Mayle et al., 2000; Burbridge et al., 2004)
8	Laguna La Gaiba ***1,3,4***	17°45.69'S	57°42.95'W	(Whitney et al., 2011; Metcalfe et al., 2014)
9*	Lagoa Silvana ***1,4***	19°31.00'S	42°25.00'W	(Rodrigues-Filho et al., 2002)
10*	Lake Dom Helvécio ***1,2,3,4***	19°46.94'S	42°35.48'W	(Ybert et al., 2000; Turcq et al., 2002; Sifeddine et al., 2004)
Size category: Medium (M)				
11	Lagoa do Caçó ***1,2,3***	2°57.64'S	43°15.20'W	(Sifeddine et al., 2003; Pessenda et al., 2005; Ledru et al., 2006)
12*	Lago Calado ***1,4***	3°16.00'S	60°35.00'W	(Behling et al., 2001b)
13	Lake Sauce ***1,2***	6°42.28'S	76°13.07'W	(Bush et al., 2016)
14	Lake Santa Rosa ***1,2***	14°28.61'S	67°52.48'W	(Urrego et al., 2013)
15	Laguna Yaguarú ***1,2,3***	15°36.00'S	63°13.00'W	(Taylor et al., 2010)
16	Lago Aleixo ***1,3,4***	17°59.27'S	42°7.13'W	(Enters et al., 2010)

1 = pollen analysis; ***2*** = charcoal analysis; ***3*** = isotopic analysis; ***4*** = physio-chemical analysis.

ID	Site Name	Latitude	Longitude	Reference(s)
17*	Lagoa Santa*1*	19°38.00'S	43°54.00'W	(Parizzi et al., 1998)
Size category: Small (S)				
18	Lake Pata*1*	0°16.00'S	66°41.00'W	(Colinvaux et al., 1996; Bush et al., 2004a)
19*	Pantano de Monica*1*	0°42.00'S	72°4.00'W	(Behling et al., 1999)
20	Maxus 4*1,2*	0°52.00'S	76°2.00'W	(Weng et al., 2002)
21	Lake Santa Maria*1,2*	1°34.76'S	53°36.41'W	(Bush et al., 2007a)
22	Lake Geral*1,2,4*	1°38.75'S	53°35.95'W	(Bush et al., 2000; 2007a)
23	Lake Saracuri*1,2*	1°40.82'S	53°34.21'W	(Bush et al., 2007a)
24*	Lake Comprida*1,2,4*	1°40.93'S	53°53.83'W	(Bush et al., 2000)
25*	Rio Curuá*1,2,4*	1°44.12'S	51°27.79'W	(Behling and da Costa, 2000)
26*	Lake Kumpaka*1*	2°50.20'S	77°57.68'W	(Liu and Colinvaux, 1988)
27	Lake Ayauchi*1,2*	3°2.72'S	78°2.07'W	(Bush and Colinvaux, 1988; McMichael et al., 2012)
28	Maranguape*1*	3°53.67'S	38°43.22'W	(Montade et al., 2014)
29*	Lake Marabá*1,2,3,4*	5°21.00'S	49°9.00'W	(Guimarães et al., 2013)
30*	Carajás CSS2*1,3,4*	6°20.51'S	50°25.16'W	(Absy et al., 1991; Sifeddine et al., 1994; 2001)
31	Lagoa da Cachoeira*1,2*	6°21.30'S	50°23.59'W	(Hermanowski et al., 2014)
32	Pántano da Maurítia*1,2,4*	6°22.55'S	50°23.16'W	(Hermanowski et al., 2012a; 2012b)
33	Humaitá HU01*1,3,4*	7°55.43'S	63°4.99'W	(Cohen et al., 2014)
34*	Saquinho*1,2*	10°24.00'S	43°13.00'W	(De Oliveira et al., 1999)
35	Lake Parker*1,2*	12°8.47'S	69°1.30'W	(Bush et al., 2007a; 2007b)
36	Lake Gentry*1,2*	12°10.64'S	69°5.86'W	(Bush et al., 2007a; 2007b)
37	Laguna Granja*1,2,5*	13°15.73'S	63°42.62'W	(Carson et al., 2014; 2015)

1 = pollen analysis; ***2*** = charcoal analysis; ***3*** = isotopic analysis; ***4*** = physio-chemical analysis.

ID	Site Name	Latitude	Longitude	Reference(s)
38	La Luna***1,2***	13°21.33'S	63°35.03'W	(Carson et al., 2016)
39	Lago Consuelo***1***	13°57.00'S	68°59.00'W	(Bush et al., 2004b)
40	Lake Chalalán***1,2***	14°25.67'S	67°55.25'W	(Urrego et al., 2013)
41	Huanchaca***2,3,5***	14°32.18'S	60°43.93'W	(Maezumi et al., 2015)
42*	Vereda de Águas Emendadas VAE2***1,2***	15°34.00'S	47°35.00'W	(Barberi et al., 2000)
43	Vereda Laçador***1***	17°49.06'S	45°26.47'W	(Cassino and Meyer, 2013)
44*	Lago do Pires***1***	17°56.85'S	42°12.62'W	(Behling, 1995a; 1998)
45	Vereda Juquinha***1***	17°56.96'S	44°15.51'W	(Pires et al., 2016)
46*	Lagoa Nova***1,2***	17°58.00'S	42°12.00'W	(Behling, 2003)
47*	Salitre de Minas***1,2,3,5***	19°0.00'S	46°46.00'W	(Ledru, 1993; Alexandre et al., 1999; Pessenda, 2004)
48	Lagoa Olhos D'Água***1***	19°38.92'S	43°54.59'W	(Raczka et al., 2013)
49	Lagoa dos Mares***1***	19°39.79'S	43°59.26'W	(Raczka et al., 2013)
50	Primeiro Rancho***1,2***	20°24.83'S	41°49.57'W	(Nuno Veríssimo et al., 2012)
51	Serra dos Órgãos***1,2***	22°27.50'S	43°1.69'W	(Behling and Safford, 2010)
52	Serra da Bocaina 2***1***	22°42.83'S	44°34.00'W	(Behling et al., 2007)
53*	Morro de Itapeva***1,2***	22°47.00'S	45°32.00'W	(Behling, 1997; 1998)
54	Colônia Crater***1***	23°52.00'S	46°42.34'W	(Ledru et al., 2005; 2009)
55*	TU Peat Bog***1***	23°59.00'S	46°44.75'W	(Pessenda et al., 2009)
56*	Serra Campos Gerais***1,2***	24°40.00'S	50°13.00'W	(Behling, 1997; 1998)
57*	Serra do Araçatuba***1,2***	25°55.00'S	48°59.00'W	(Behling, 2007)
58	Volta Velha***1***	26°4.00'S	48°37.98'W	(Behling and Negrelle, 2001)
59*	Serra da Boa Vista***1***	27°42.00'S	49°9.00'W	(Behling, 1995b; 1998)
60	Serra do Tabuleiro***1,2***	27°53.81'S	48°52.09'W	(Jeske-Pieruschka et al., 2012)

1 = pollen analysis; ***2*** = charcoal analysis; ***3*** = isotopic analysis; ***4*** = physio-chemical analysis.

ID	Site Name	Latitude	Longitude	Reference(s)
61*	Morro da Igreja[1]	28°11.00'S	49°52.00'W	(Behling, 1995b; 1998)
62*	Serra do Rio Rostro[1]	28°23.00'S	49°33.00'W	(Behling, 1995b; 1998)
63	Cambará do Sul[1,2]	29°3.15'S	50°6.07'W	(Behling et al., 2004; Behling and Pillar, 2007)
64*	Fazenda do Pinto[1]	29°24.00'S	50°34.00'W	(Behling et al., 2001a)
65	Rincão das Cabritas[1,2]	29°28.58'S	50°34.37'W	(Jeske-Pieruschka and Behling, 2011)
66	Alpes de São Francisco[1]	29°29.59'S	50°37.30'W	(Leonhardt and Lorscheitter, 2010)
67	Itajuru Farm[1,2]	29°35.20'S	55°13.03'W	(Behling et al., 2005)
68*	Serra Velha[1]	29°36.37'S	51°38.92'W	(Leal and Lorscheitter, 2007)
69	Santo Antônio da Patrulha[1,2]	29°44.75'S	50°32.93'W	(Macedo et al., 2010)
Size category: Extra small (XS)				
70	Combination of soil profiles: C17, C20, C25, C54, F15[2,3]	2°45.00'S	43°0.00'W	(Pessenda et al., 2004; 2005)
71	Combination of soil profiles: F46, C78[2,3]	3°12.00'S	43°5.33'W	(Pessenda et al., 2004)
72	Combination of soil profiles: LCF50, LCF150, LCF200[3]	2°57.98'S	43°16.03'W	(Pessenda et al., 2004; 2005)
73	Combination of soil profiles: Parna I, Parna IV[2,3]	4°5.69'S	41°43.71'W	(Pessenda et al., 2010)
74	Combination of soil profiles: Parna II, Parna VII[2,3]	4°7.81'S	41°42.65'W	(Pessenda et al., 2010)
75	Combination of soil profiles: Parna III, Parna V, Parna VI, Parna VIII[2,3]	4°4.45'S	41°41.17'W	(Pessenda et al., 2010)
76	Combination of soil profiles: Rebio I, Rebio II, Rebio III,	6°47.79'S	35°5.98'W	(Pessenda et al., 2010)

1 = pollen analysis; ***2*** = charcoal analysis; ***3*** = isotopic analysis; ***4*** = physio-chemical analysis.

ID	Site Name	Latitude	Longitude	Reference(s)
	Rebio IV[2,3]			
77	Combination of soil profiles: Rebio V, Rebio VI, Rebio VII, Rebio VIII[2,3]	6°41.42'S	35°9.67'W	(Pessenda et al., 2010)
78	Combination of soil profiles: Flona km4, Flona km8[2,3]	7°19.20'S	39°28.20'W	(Pessenda et al., 2010)
79	Combination of soil profiles: Flona km6', Flona km12'[2,3]	7°15.00'S	39°33.00'W	(Pessenda et al., 2010)
80	Combination of soil profiles: Flona km0, Flona km0'[2,3]	7°15.00'S	39°28.20'W	(Pessenda et al., 2010)
81	Combination of soil profiles: BR319 km178.5, BR319 km179[3]	7°37.80'S	63°0.00'W	(de Freitas et al., 2001)
82	Combination of soil profiles: BR319 km154, BR319 km188[3]	7°47.00'S	63°9.00'W	(de Freitas et al., 2001)
83	Combination of soil profiles: BR319 km80, BR319 km82, Humaitá C, Humaitá D[3]	8°10.00'S	63°48.00'W	(de Freitas et al., 2001)
84	Combination of soil profiles: BR319 km100, BR319 km111, BR319 km142, BR319 km161[3]	8°3.00'S	63°31.00'W	(de Freitas et al., 2001)
85	Combination of soil profiles: BR319 km46, BR319 km68, Humaitá A, Humaitá B, Humaitá E[3]	8°30.00'S	63°58.00'W	(de Freitas et al., 2001)
86	BR319 km5[3]	8°43.00'S	63°58.00'W	(de Freitas et al., 2001)
87	Ariquemes[3]	10°10.00'S	62°49.00'W	(Pessenda et al., 1998)
88	Pimenta Bueno - forest[3]	11°46.00'S	61°15.00'W	(Pessenda et al., 1998)

1 = pollen analysis; ***2*** = charcoal analysis; ***3*** = isotopic analysis; ***4*** = physio-chemical analysis.

ID	Site Name	Latitude	Longitude	Reference(s)
89	Pimenta Bueno - cerradão*3*	11°49.00'S	61°10.00'W	(Pessenda et al., 1998)
90	Vilhena*3*	12°42.00'S	60°7.00'W	(Pessenda et al., 1998)
91	Pontes e Lacerda*2,3*	15°16.00'S	59°13.00'W	(Gouveia et al., 2002)
92	Pitoco*3*	15°55.87'S	47°52.61'W	(Silva et al., 2008)
93	Taquara*3*	15°57.22'S	47°53.32'W	(Silva et al., 2008)
94	Laguna Sucuara*3,4*	16°49.60'S	62°2.60'W	(Zech et al., 2009)
95	Pau-de-Fruta*3,4*	18°15.45'S	43°40.06'W	(Horák et al., 2011)
96	Machado soil core*3,5*	21°40.70'S	45°55.45'W	(Calegari et al., 2013)
97	Jaguariúna*2,3*	22°40.00'S	47°1.00'W	(Gouveia et al., 2002; Pessenda, 2004)
98	Piracicaba*2,3*	22°43.00'S	47°38.00'W	(Pessenda, 2004)
99	Anhembi*2,3*	22°45.00'S	47°58.00'W	(Gouveia et al., 2002; Pessenda, 2004)
100	Botucatu*2,3*	23°0.00'S	48°0.00'W	(Gouveia et al., 2002; Pessenda, 2004)
101	Londrina*2,3*	23°18.00'S	51°10.00'W	(Pessenda, 2004)
102	Combination of soil profiles: CER1, CER2, PCN, LN, AC, AF, FSM, EG, EG*3*	24°0.15'S	46°45.97'W	(Pessenda et al., 2009)
103	Saibadela*3*	24°14.42'S	48°4.87'W	(Saia et al., 2008)
104	Bairro Lajeado*3*	24°18.31'S	48°21.91'W	(Saia et al., 2008)
105	Base do Carmo*3*	24°18.41'S	48°24.86'W	(Saia et al., 2008)
106	Bulha D'Água*3*	24°20.25'S	48°30.15'W	(Saia et al., 2008)
107	Bairro Camargo Baixo*3*	24°32.53'S	48°39.19'W	(Saia et al., 2008)
108	Iporanga*3*	24°33.32'S	48°39.45'W	(Saia et al., 2008)
109	Misiones*3,4*	27°23.40'S	55°31.50'W	(Morrás et al., 2009; Zech et al., 2009)

1 = pollen analysis; ***2*** = charcoal analysis; ***3*** = isotopic analysis; ***4*** = physio-chemical analysis.

ID	Site Name	Latitude	Longitude	Reference(s)
110	Centro de Pesquisas e Conservação da Natureza*3*	29°28.48'S	50°9.79'W	(Dümig et al., 2008)

1 = pollen analysis; ***2*** = charcoal analysis; ***3*** = isotopic analysis; ***4*** = physio-chemical analysis.

Table 2.

Code	Vegetation classification	Description
HETF	Humid evergreen tropical forest	Tall, closed canopy evergreen forest occurring in climates of > ~1600 mm annual precipitation. Can occur in seasonal conditions with dry season length < ~ 4 months.
SDF	Semi-deciduous tropical forest	Shorter trees, varying canopy cover, deciduous/semi-deciduous drought adapted taxa common, < ~1600 mm annual precipitation, marked dry season of 5 – 6 months
GAL	Gallery forest	Occur along streams and rivers where moisture levels can be maintained
ARF	Araucaria forest	Exist on high elevations (500 – 1800 m) under moist conditions, annual precipitation ~2000 mm and a short or no marked dry season
CLF	Cloud/montane forest	Mostly evergreen, closed forests with medium sized trees and shrubs, existing at high elevations (> ~ 1000 m), where orographic rain and persistent low-level clouds can maintain moisture levels
SAV	Savannah/ Grassland/ Scrubland	Generally, refers to open savannahs with few arboreal elements indicative of low annual precipitation (< ~1500 mm) and a long dry season (> 5 – 6 months). We also include sub-tropical campos grassland in this classification to represent open vegetation on the south Brazilian highlands that can exist in climates with dry season lengths ~ 3 months.

Code	Vegetation classification	Description
PSW	Palm swamp	Flooded, wetland areas (often due to poor soil drainage), often dominated by the palm *Mauritia flexuosa*

Table 3.

Category	**Definition**
Large (L)	Lakes larger than ~5 km^2, vegetation reconstructions representative of regional scale
Medium (M)	Lakes between ~800 m^2 and 5 km^2, vegetation reconstructions representative of local to regional scale
Small (S)	Peat bogs, terrestrial swamps, lakes less than 800 m^2, vegetation reconstructions representative of local scale
Extra-small (XS)	Soil pits, representative of point-scale (i.e. wherever the pit was taken)

Impact of mid-to-late Holocene precipitation changes on vegetation across lowland tropical South America: a palaeo-data synthesis:

Authors: Richard J. Smith and Francis E. Mayle

Supplementary Information

Figure S1. Summary tables of vegetation changes at each palaeoecological site, alongside regional maps of the location of each site. Site IDs correspond to those in Table 1.

(a) Central and western lowland Amazonia

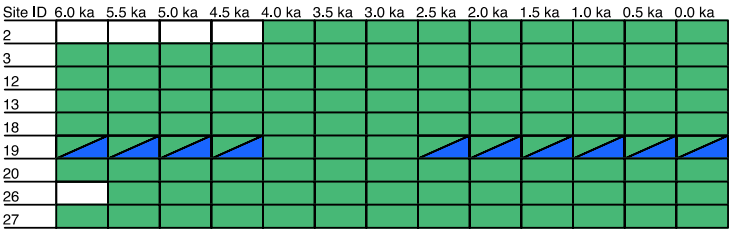

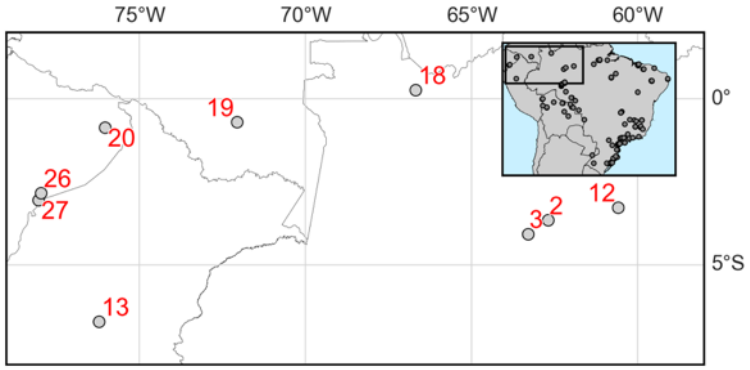

(b) South-Western Amazonia

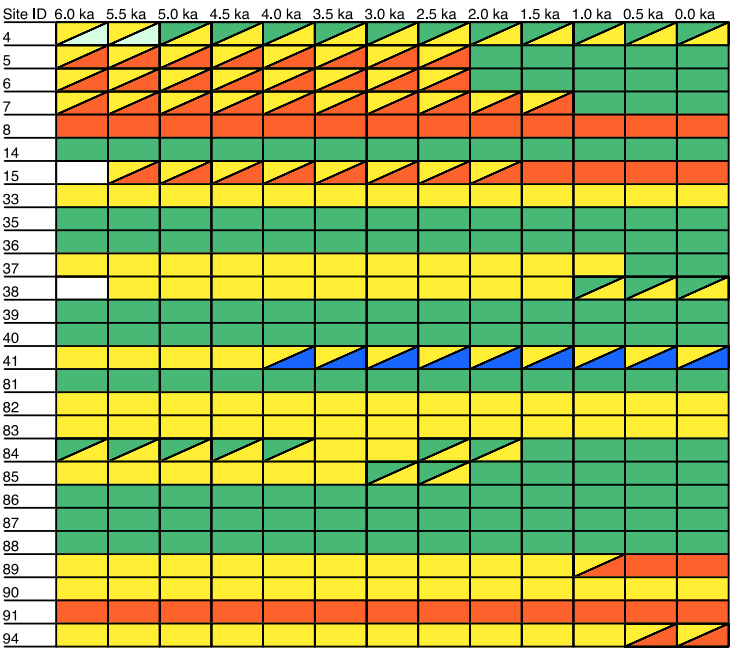

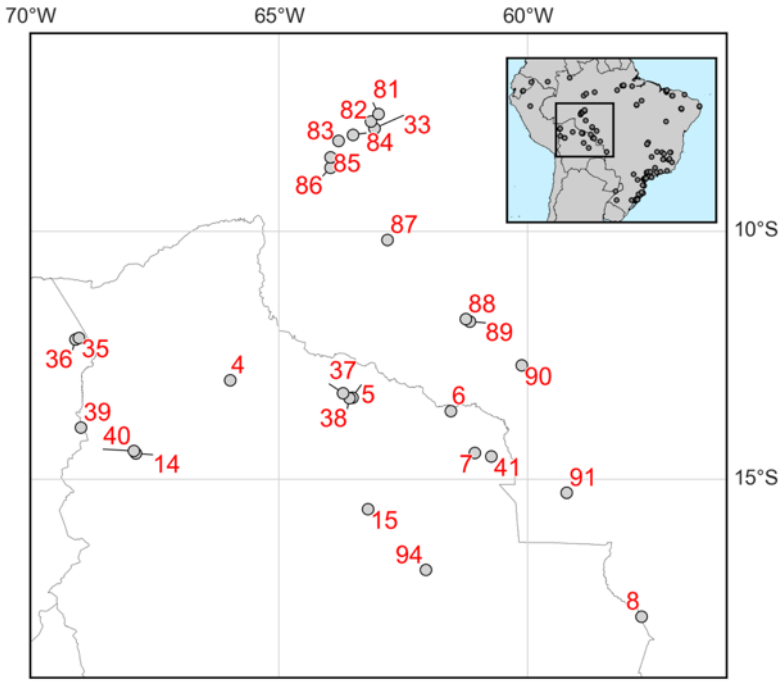

(c) South-eastern Brazil

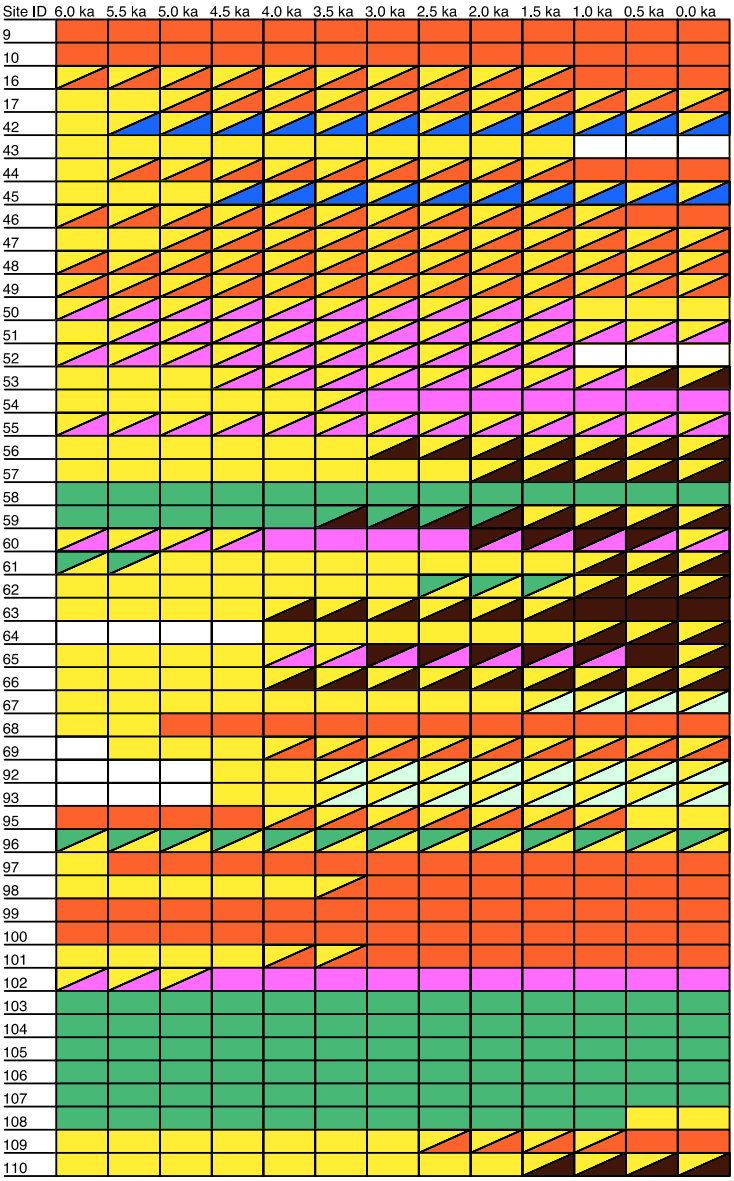

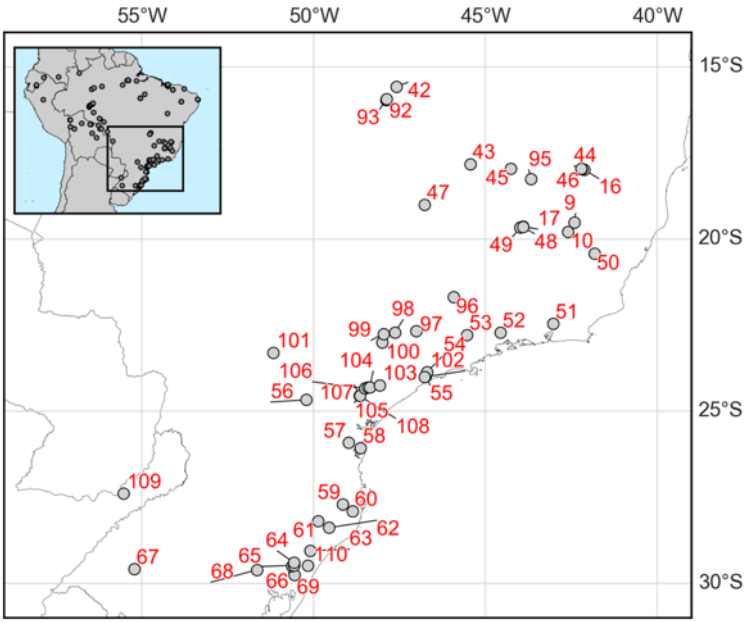

(d) Eastern Amazonia

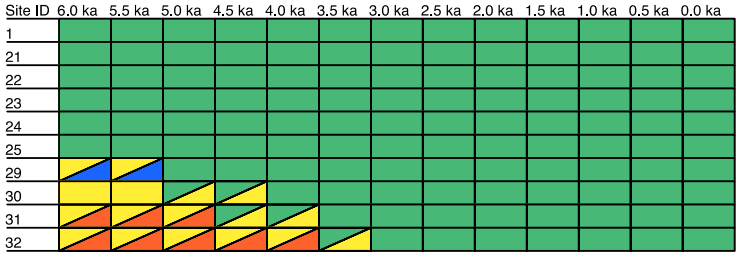

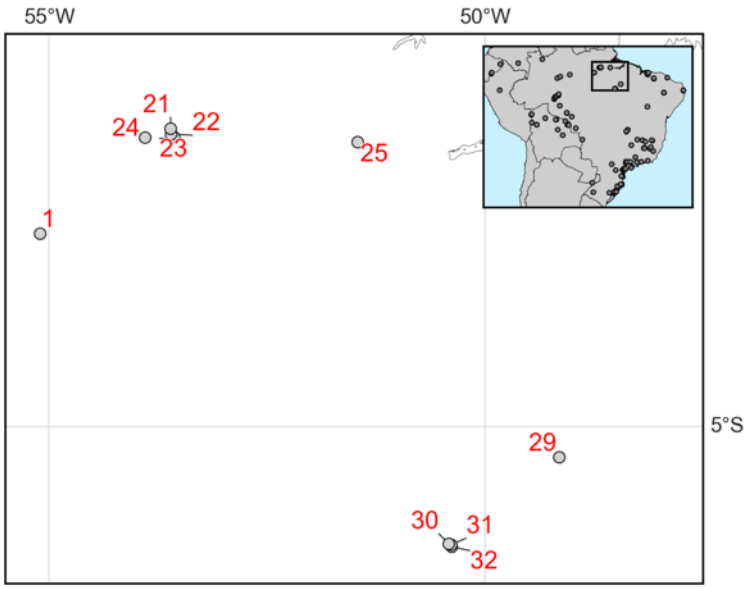

(e) North-eastern Brazil

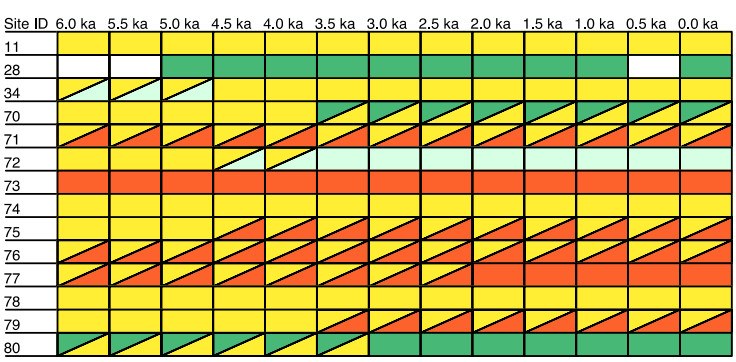

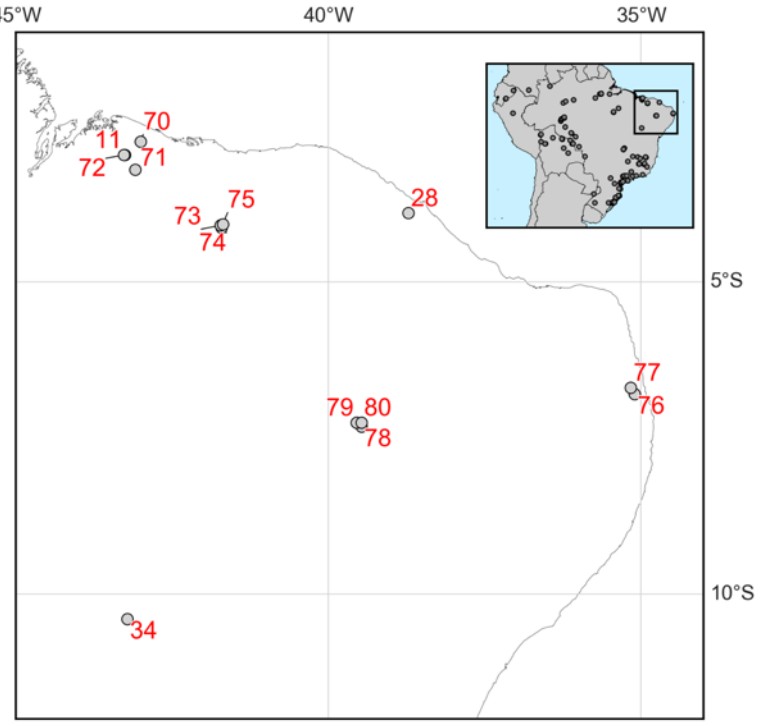

Palaeoecological classifications

- Humid Evergreen Tropical Forest
- Savannah/Grassland/Scrubland
- Gallery Forest
- Semi-deciduous tropical forest
- Cloud/Montane Forest
- Araucaria forest
- Palm Swamp